

UCLA Dark Matter 2023

The search for Light Dark Matter with NEWS-G

Daniel Durnford

On behalf of the NEWS-G Collaboration

Supervisor: Marie-Cécile Piro

March 30th 2023



**UNIVERSITY
OF ALBERTA**



CFI FCI

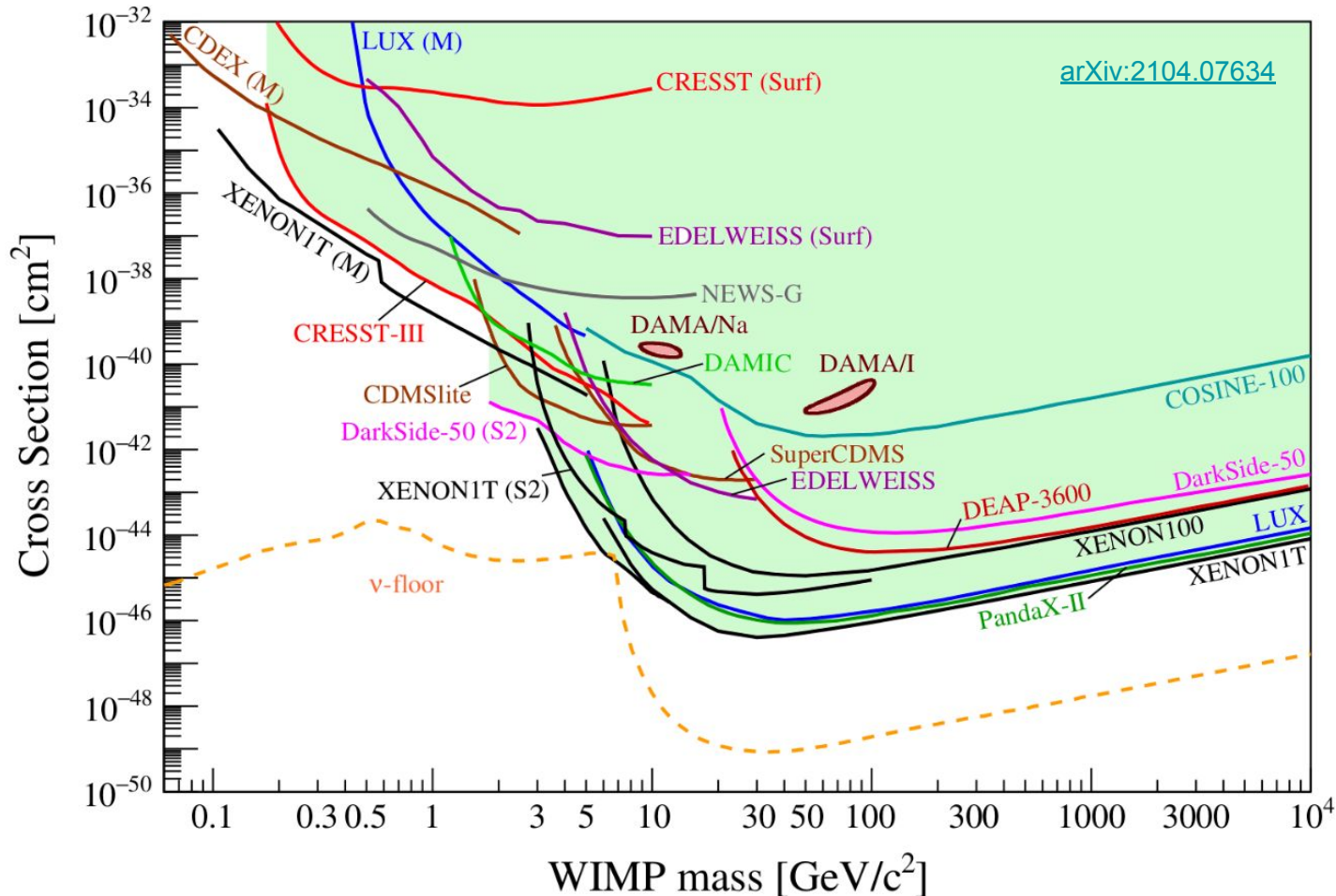


**NSERC
CRSNG**

Direct detection of dark matter



Absence of canonical WIMPs [1,2] motivates searches for other low mass WIMP-like DM candidates [3,4]



[1] D. Bauer et al, Phys. Dark Univ., 7–8, 16–23 (2015)

[2] K. Petraki et al, Int. J. Mod. Phys. A, 28(19), 1330028 (2013)

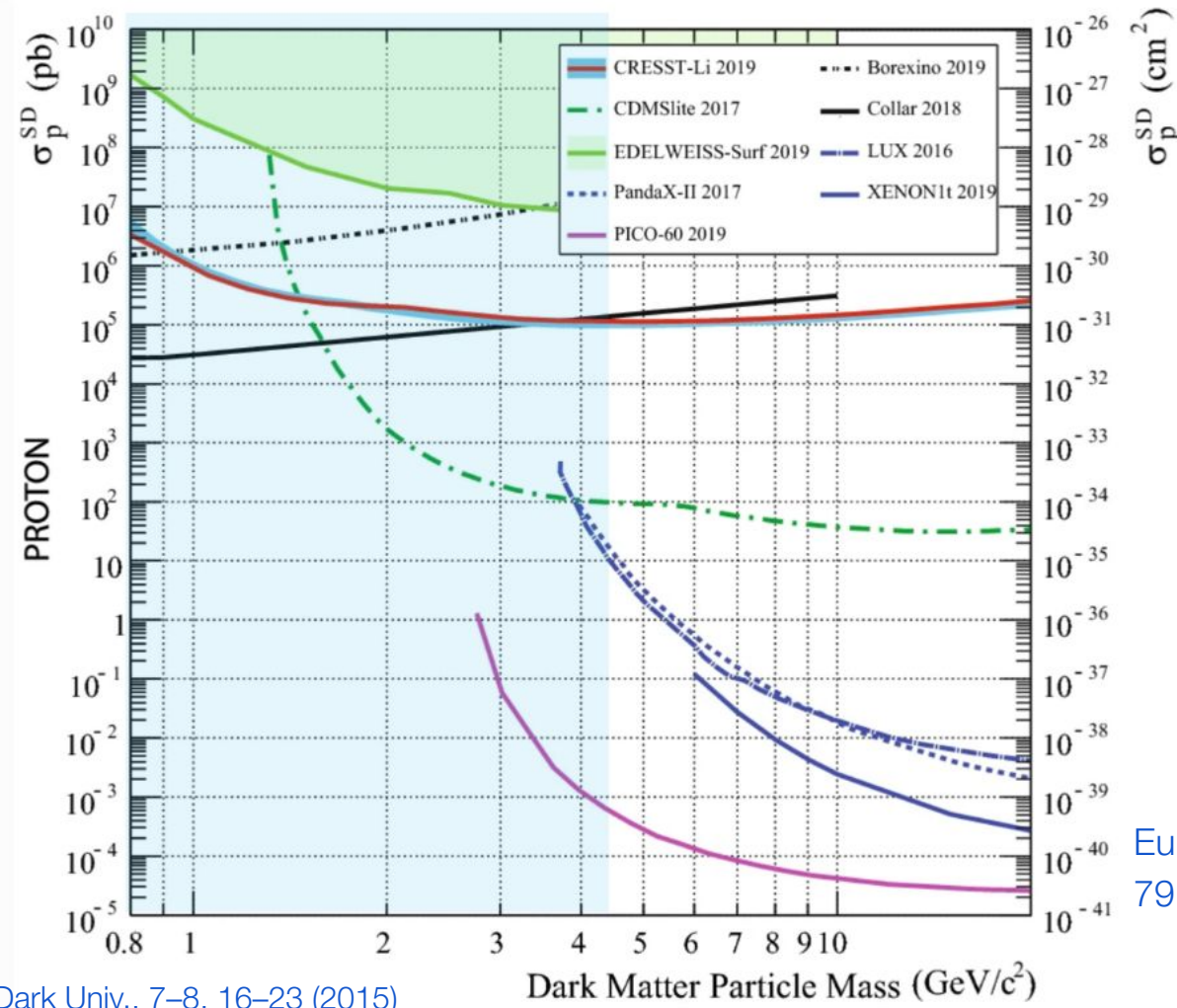
[3] K.M. Zurek, Phys. Rep., 537(3), 91 (2014)

[4] R. Essig et al, Dark Sectors and New, Light, Weakly-Coupled Particles (2013)

Direct detection of dark matter



Absence of canonical WIMPs [1,2] motivates searches for other low mass WIMP-like DM candidates [3,4]



Eur. Phys. J. C
79, 630 (2019)

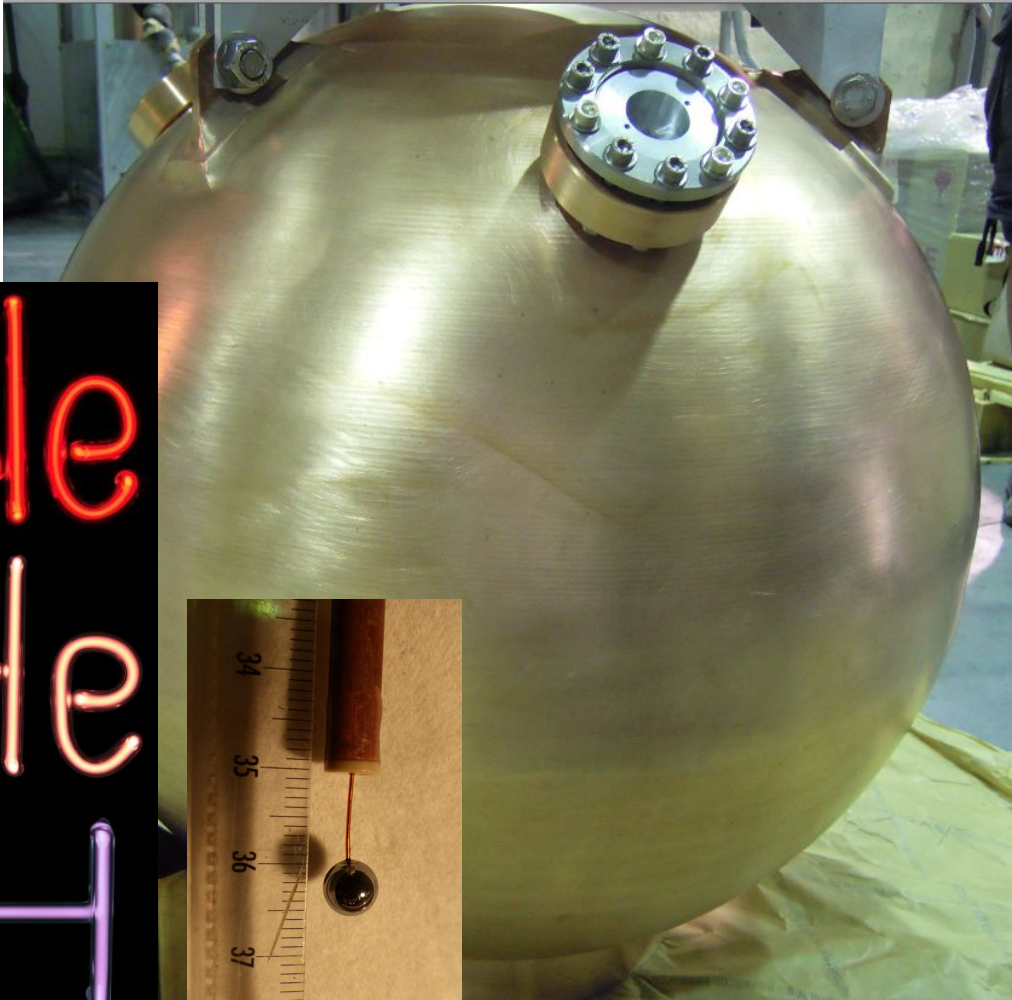
[1] D. Bauer et al, Phys. Dark Univ., 7–8, 16–23 (2015)

[2] K. Petraki et al, Int. J. Mod. Phys. A, 28(19), 1330028 (2013)

[3] K.M. Zurek, Phys. Rep., 537(3), 91 (2014)

[4] R. Essig et al, Dark Sectors and New, Light, Weakly-Coupled Particles (2013)

Spherical Proportional Counters (SPCs) to search for low-mass dark matter



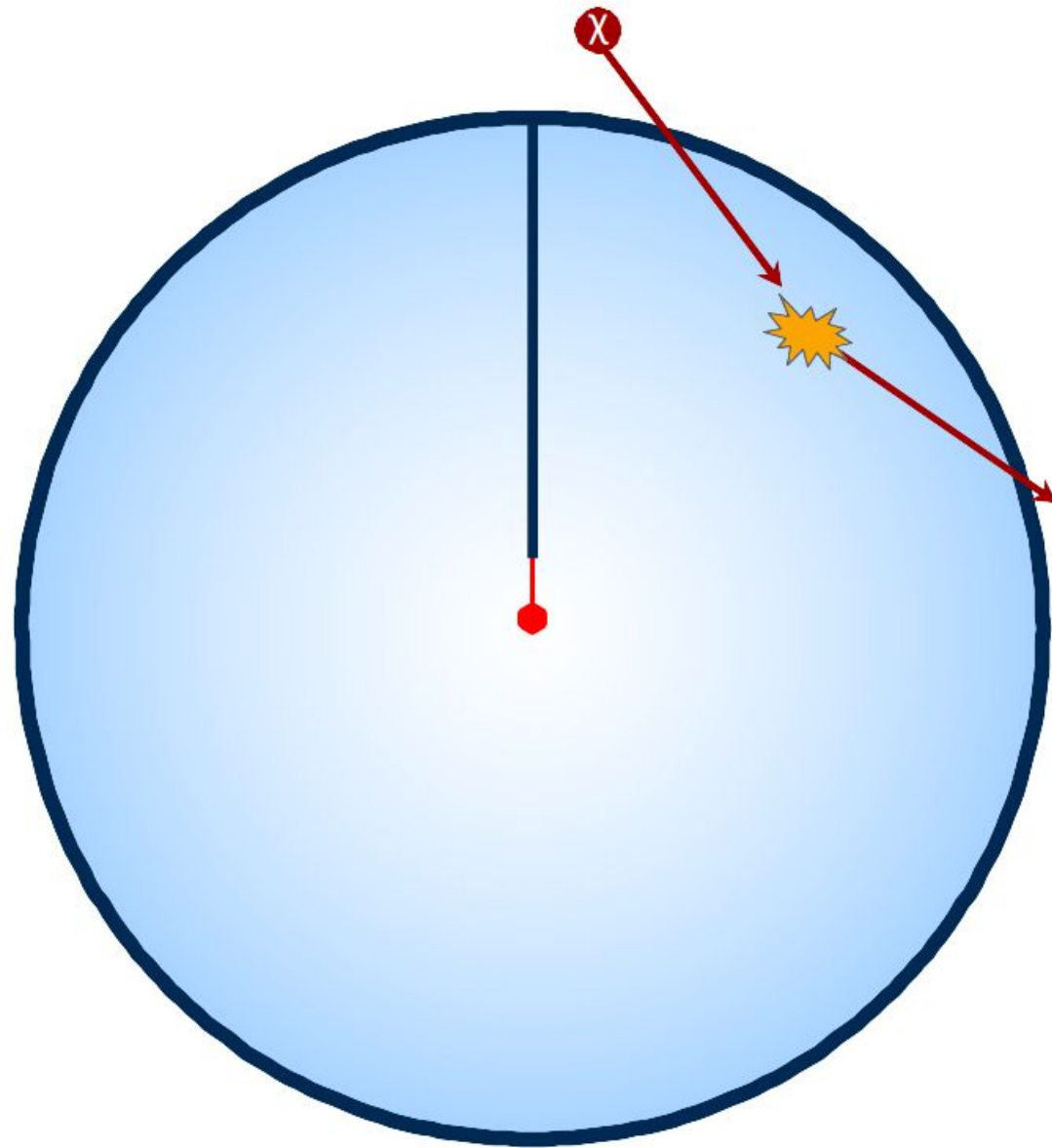
Metallic vessel filled with a noble gas mixture, with a single high voltage anode/sensor

Low-A target atoms increases sensitivity to low-mass dark matter

Low capacitance (~ 10 pF) decreases electronic baseline noise

Townsend avalanche provides large gain

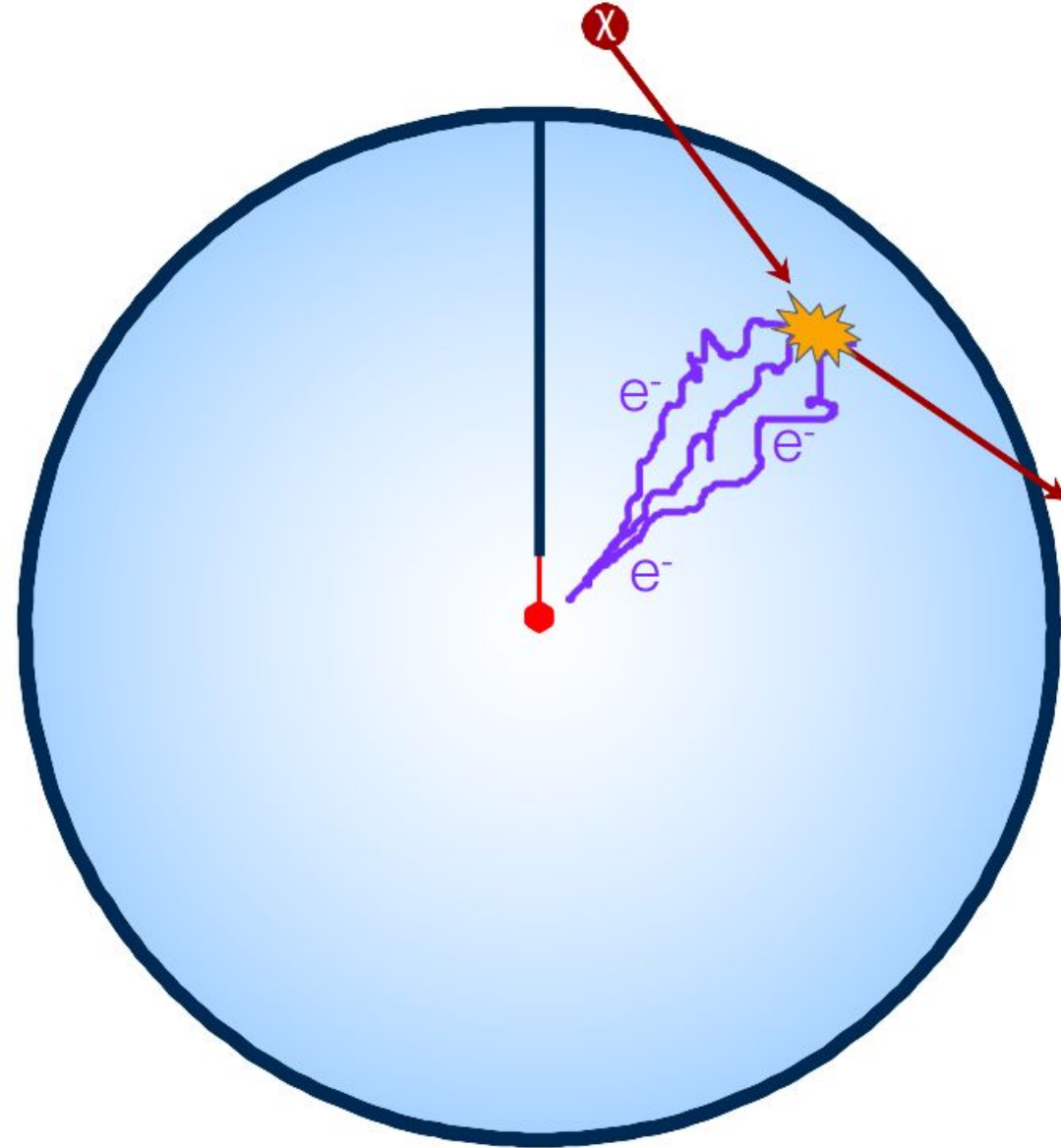
Single ionization detection threshold!



(1) Primary Ionization

$$\langle \#PE \rangle = \frac{E}{W(E)}$$

$$W_{nr} = W_{\gamma}/Q(E) \quad \text{Neon: } W_{\gamma} \sim 36 \text{ eV/pair} \\ Q \sim 0.2$$



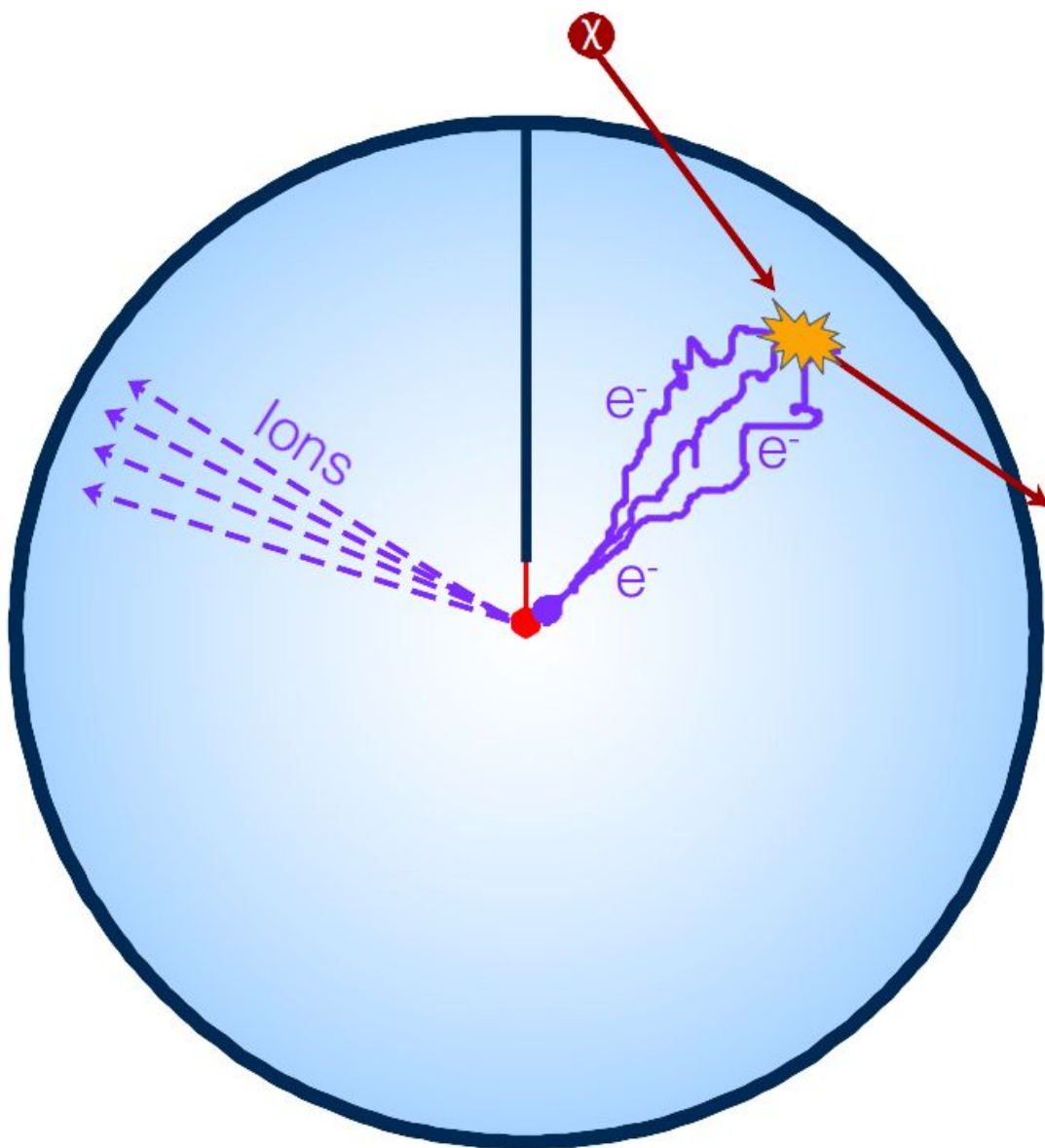
(1) Primary Ionization

$$\langle \#PE \rangle = \frac{E}{W(E)}$$

$$W_{nr} = W_{\gamma}/Q(E) \quad \text{Neon: } W_{\gamma} \sim 36 \text{ eV/pair} \\ Q \sim 0.2$$

(2) Drift of charges

Radially-dependent diffusion allows for fiducialization



(1) Primary Ionization

$$\langle \#PE \rangle = \frac{E}{W(E)}$$

$$W_{nr} = W_{\gamma}/Q(E) \quad \text{Neon: } W_{\gamma} \sim 36 \text{ eV/pair} \\ Q \sim 0.2$$

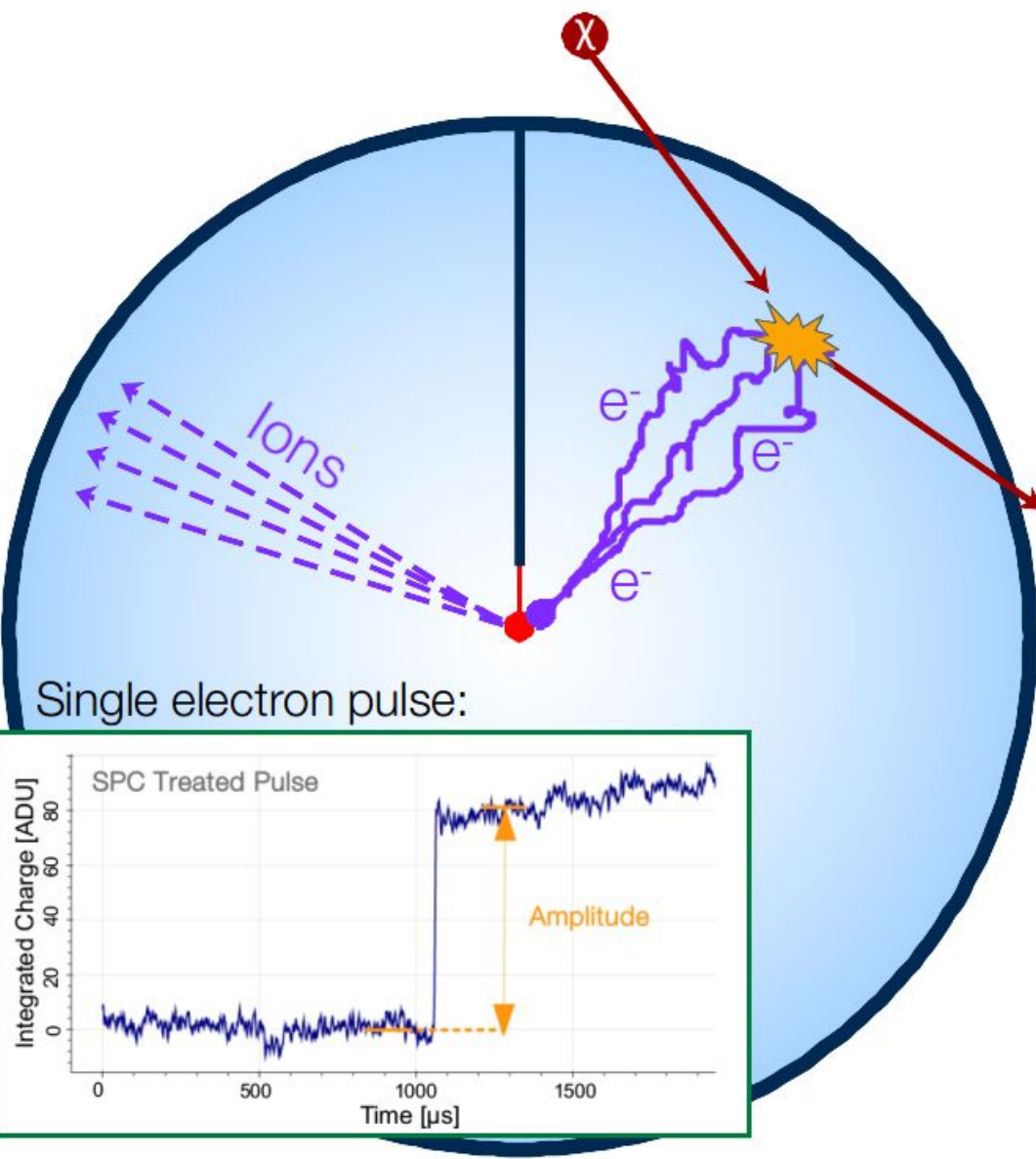
(2) Drift of charges

Radially-dependent diffusion allows for fiducialization

(3) Avalanche of secondary e⁻/ion pairs

Amplification of signal through Townsend avalanche (tunable with V)

(~10³ - 10⁴ secondary pairs)



(1) Primary Ionization

$$\langle \#PE \rangle = \frac{E}{W(E)}$$

$$W_{nr} = W_{\gamma}/Q(E) \quad \text{Neon: } W_{\gamma} \sim 36 \text{ eV/pair} \\ Q \sim 0.2$$

(2) Drift of charges

Radially-dependent diffusion allows for fiducialization

(3) Avalanche of secondary e^- /ion pairs

Amplification of signal through Townsend avalanche (tunable with V)

(4) Signal formation

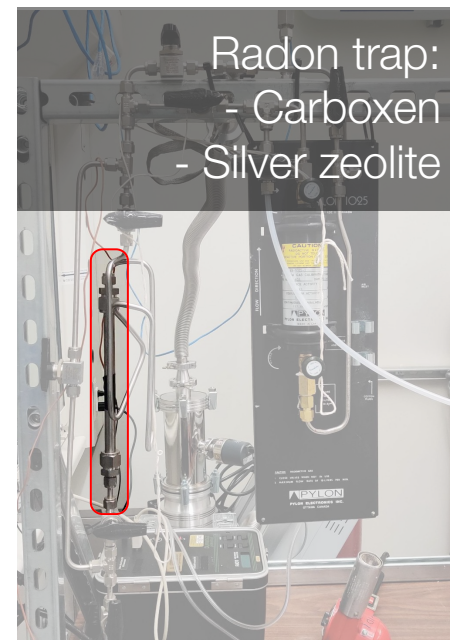
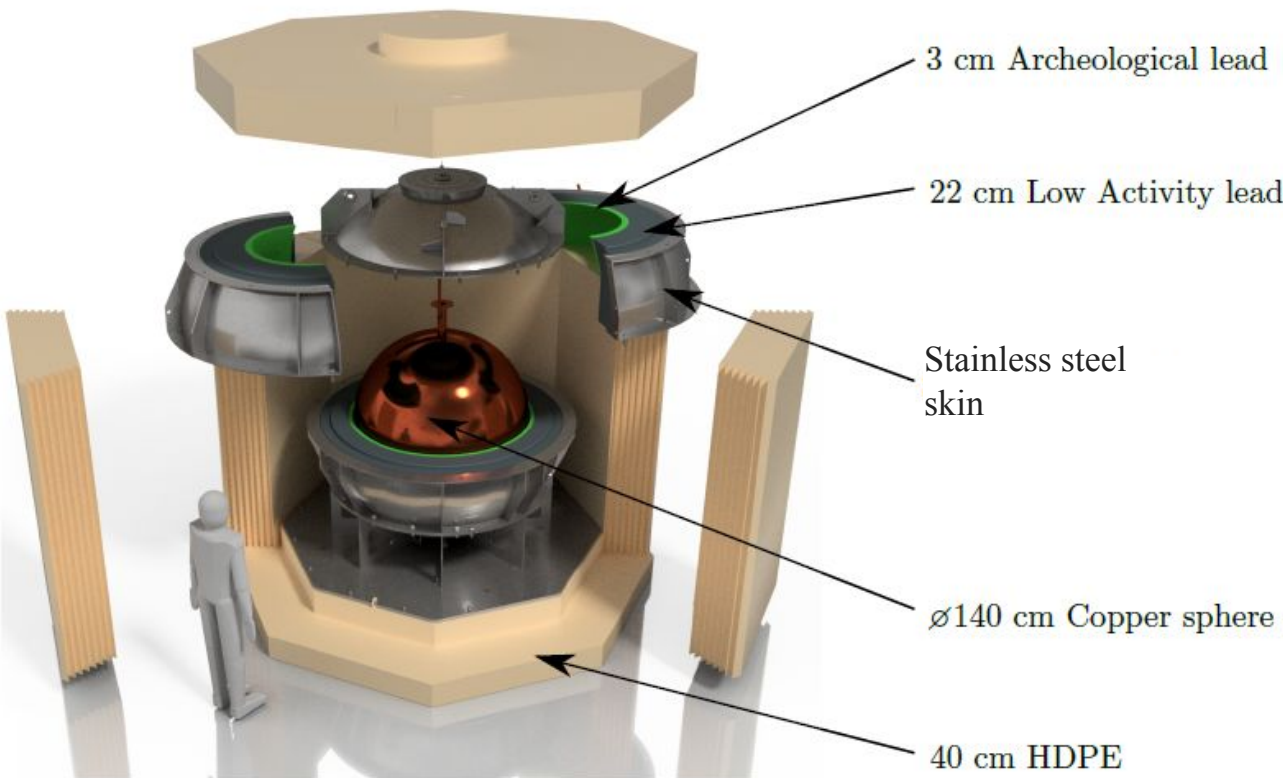
Current induced by the secondary ions drifting away from anode

(5) Signal readout

Current integrated and digitized

The S140 detector

- Radio-pure construction, multi-layered compact shield system
- Gas quality: contamination filter and radon removal, precise measurement of methane
- Multi-anode sensor for more isotropic response, stronger drift field
- 0.5mm electroplated copper interior to shield Pb-210 Brem [1,2]



I. Katsioulas, Journal of Physics: Conference Series 1468 (2020) 0122058



1. K. Abe *et al*, Nucl. Instrumen. Methods A, 884 (2018)
2. L. Balogh *et al*, Nucl. Instrumen. Methods A, 988 (2021)

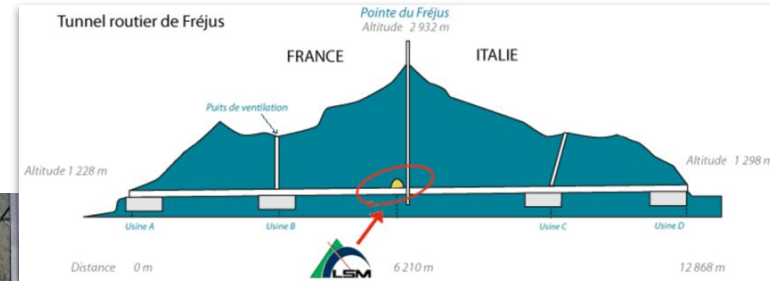
Commissioning data was taken at the LSM:



A water tank was used instead of the PE shield. First test of sensor deployment system, electronics

~10 days of data taken with 135 mbar of pure CH_4 (110 g):

- Larger fraction of hydrogen for low-mass DM sensitivity
- More transparent to high energy γ 's, lower background rate/unit mass than Ne/CH_4 mixture

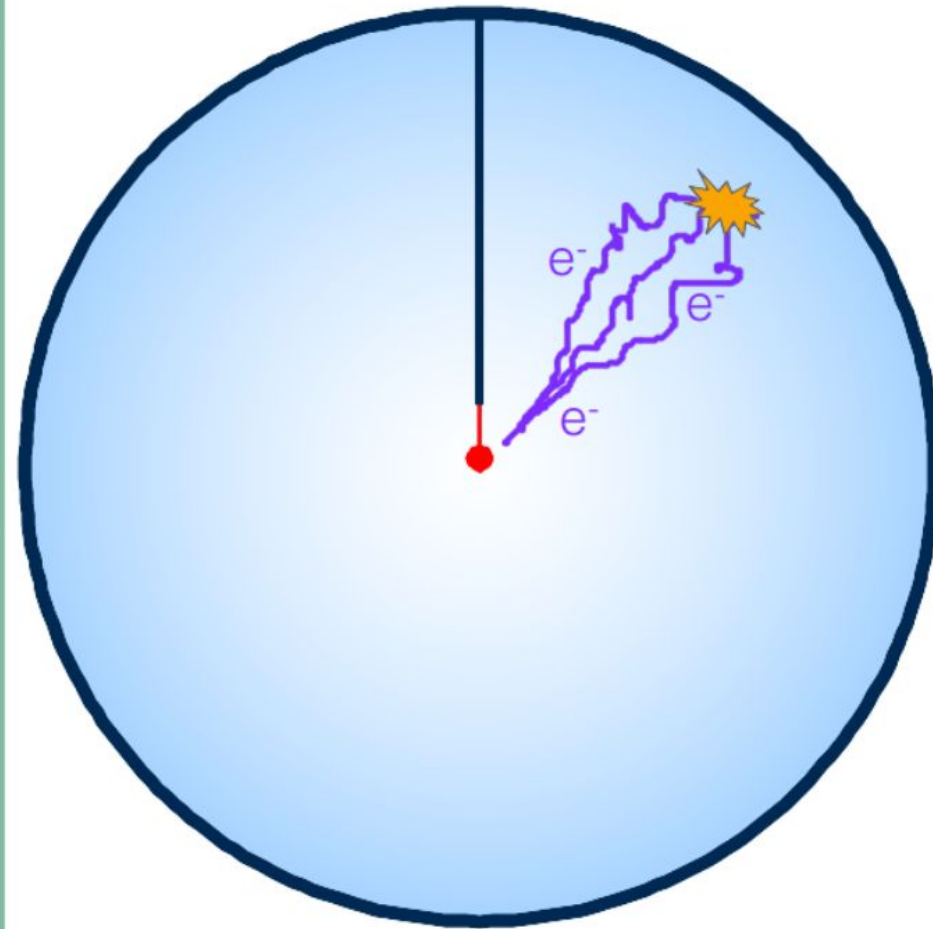
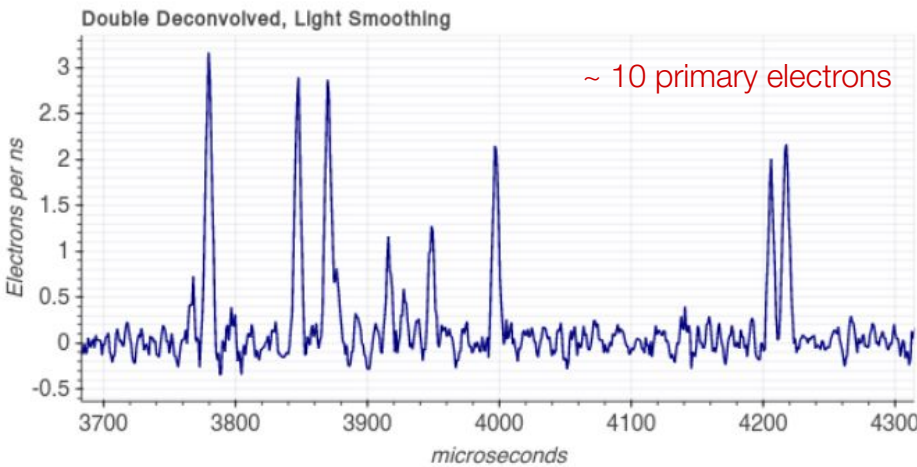
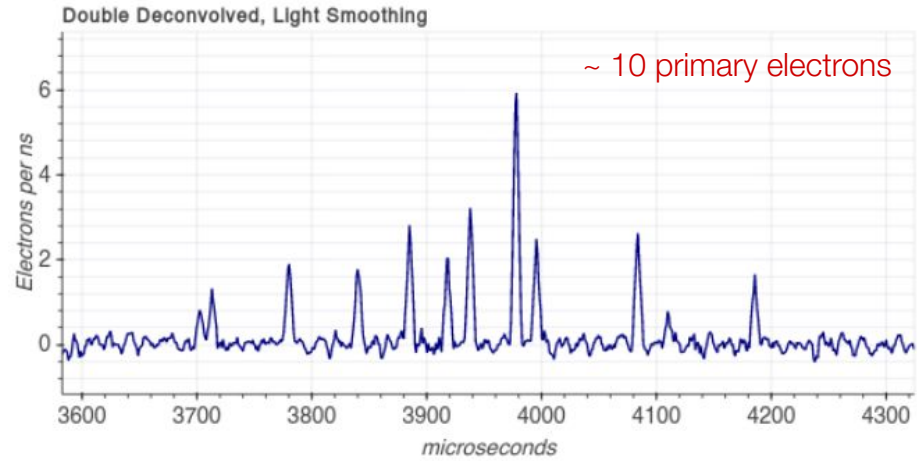


Electron peak finding



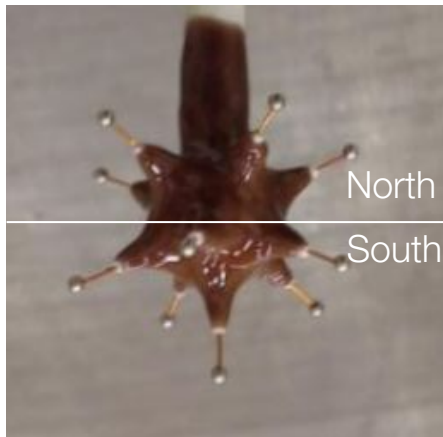
The large drift volume allows us to resolve individual primary electrons in time!

UV Laser events from new 140cm SPC:

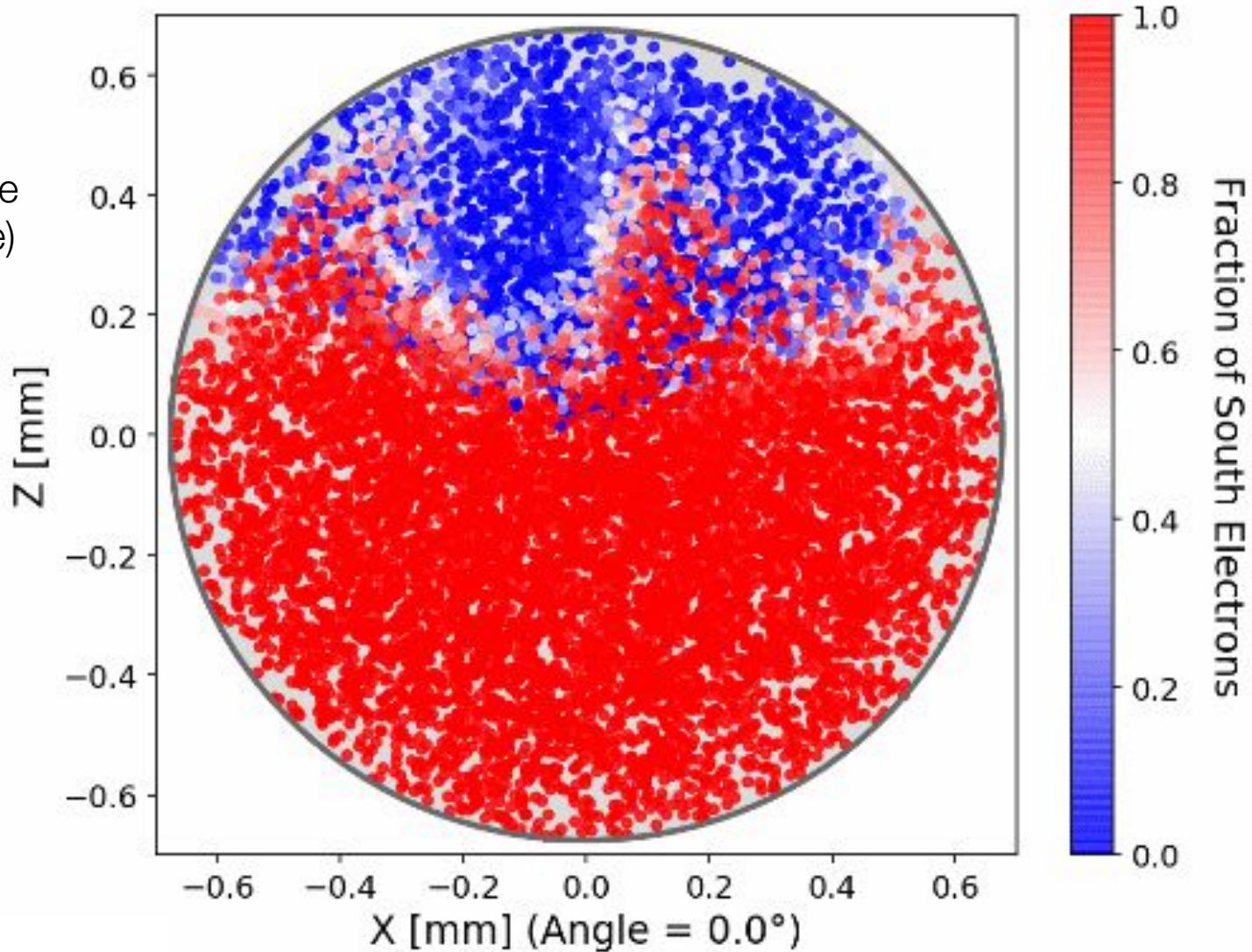


The 11-anode sensor is read out in two channels (north and south)

In this analysis, only pure south-channel events are kept as candidate events (more isotropic field structure)



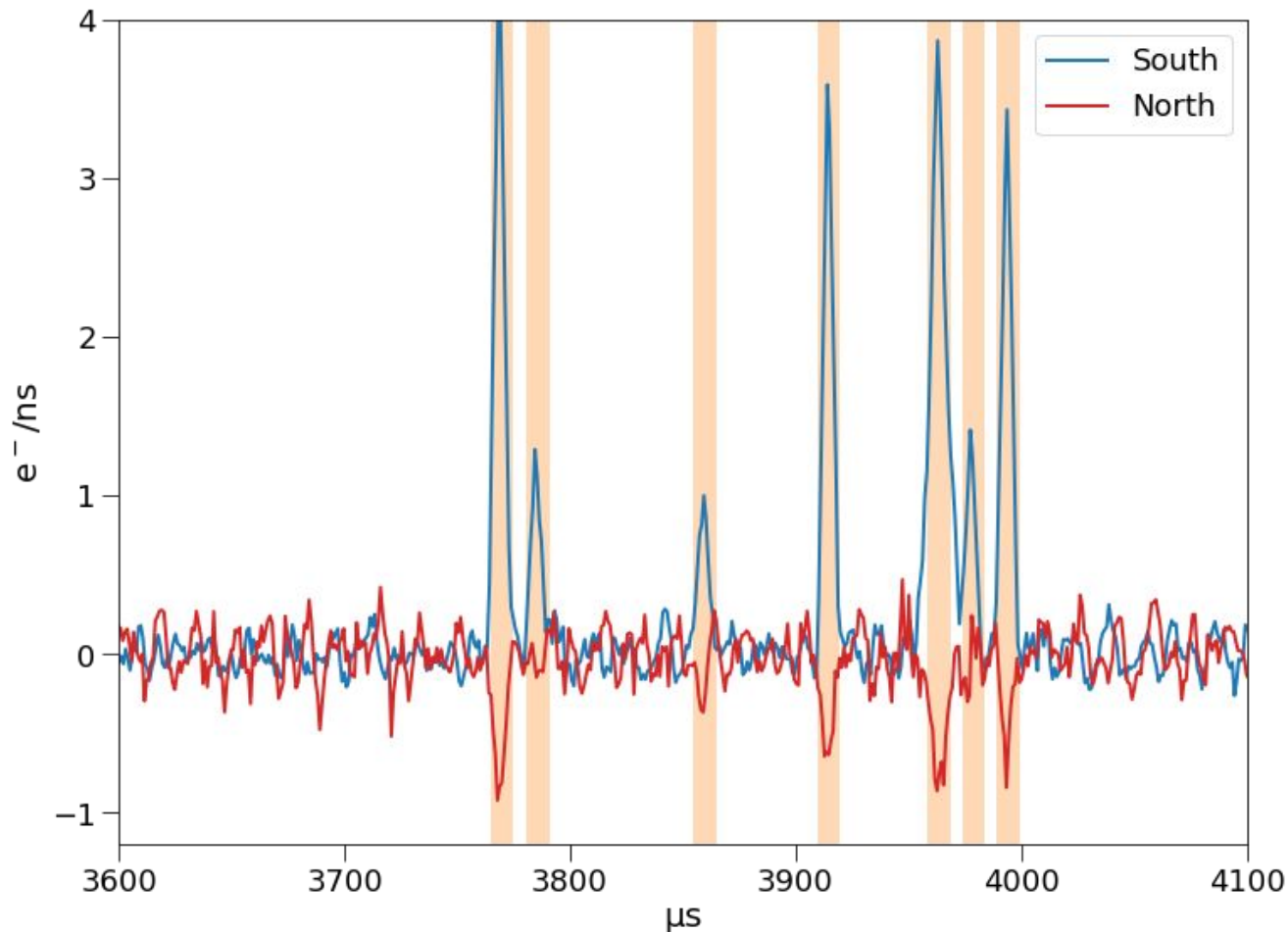
The fiducial volume covered by the southern 6 anodes is approximately 70%

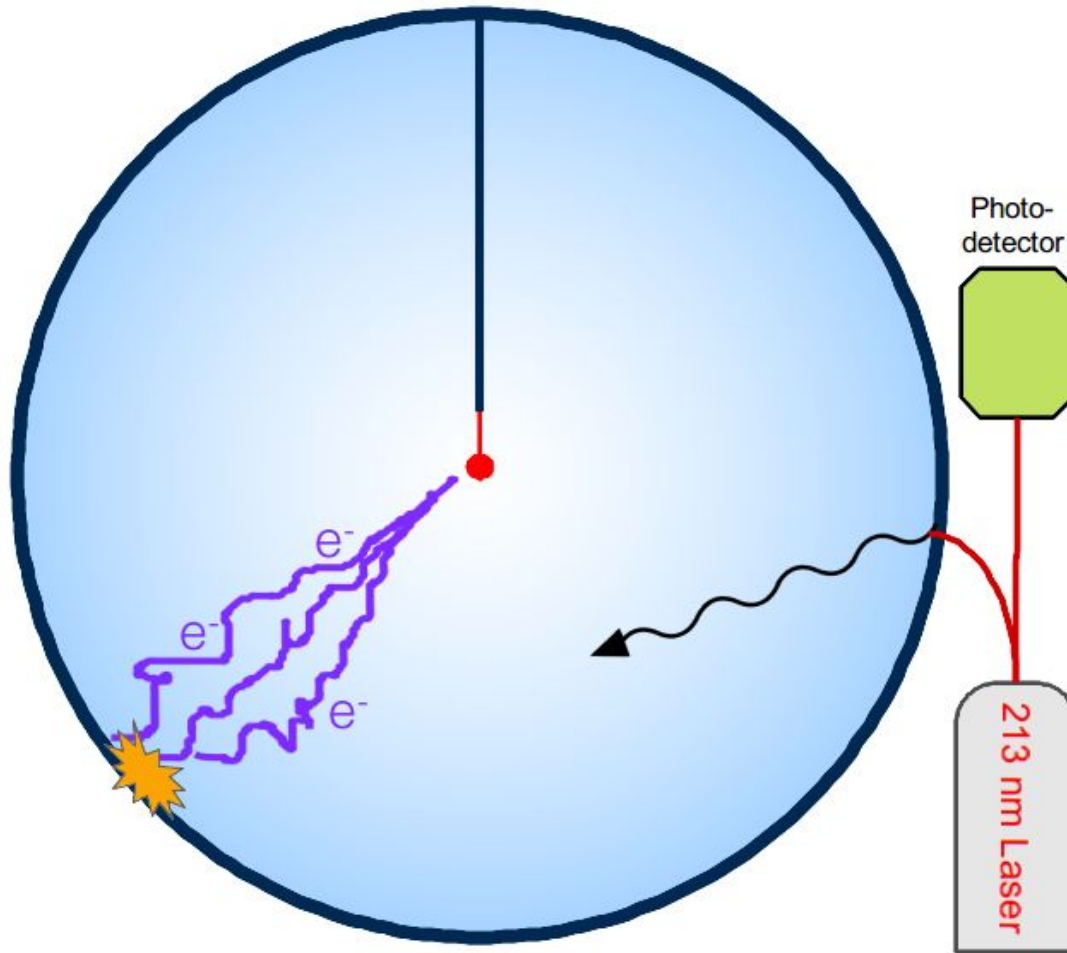


Physical events induce mirror, smaller pulses in the opposite sensor channel with a characteristic scale

Spurious pulses (electronic artifacts) do not exhibit this behaviour, and tend to be sharper

PSD possible using combination of North/South peak amplitudes and pulse derivative: 77% of physical events kept, 95% of spurious pulses rejected





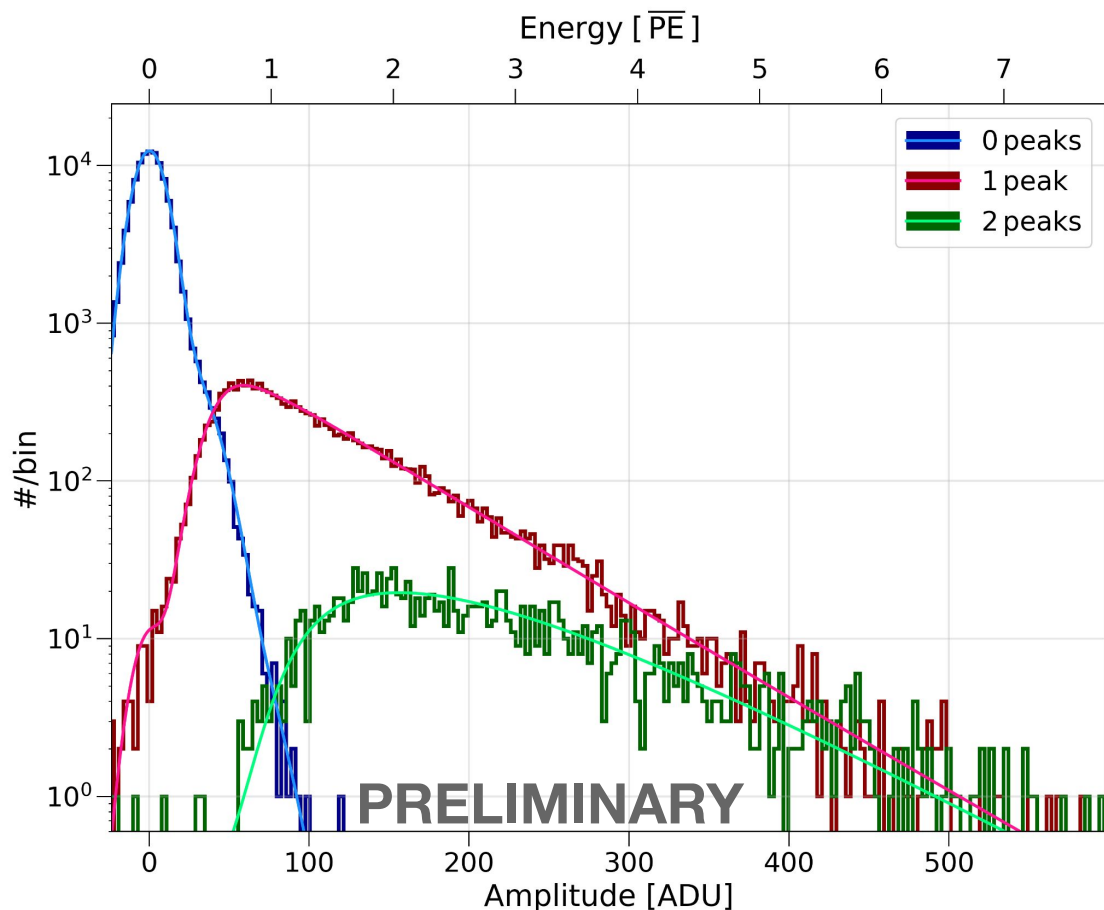
A 213 nm laser shone into the sphere extracts photo-electrons from the inner surface of the vessel [1]:

Laser-induced calibration events are tagged with a photodiode

Continuous operation during physics runs allows for monitoring of the detector response

Low intensity laser data also allows for measurement of the hardware trigger efficiency

[1] Q. Arnaud et al, Phys. Rev. D 99, 102003 (2019)



A 213 nm laser shone into the sphere extracts photo-electrons from the inner surface of the vessel [1]:

Data with 0 or a few electrons is used to measure the single electron response of the detector (gain and avalanche statistics)

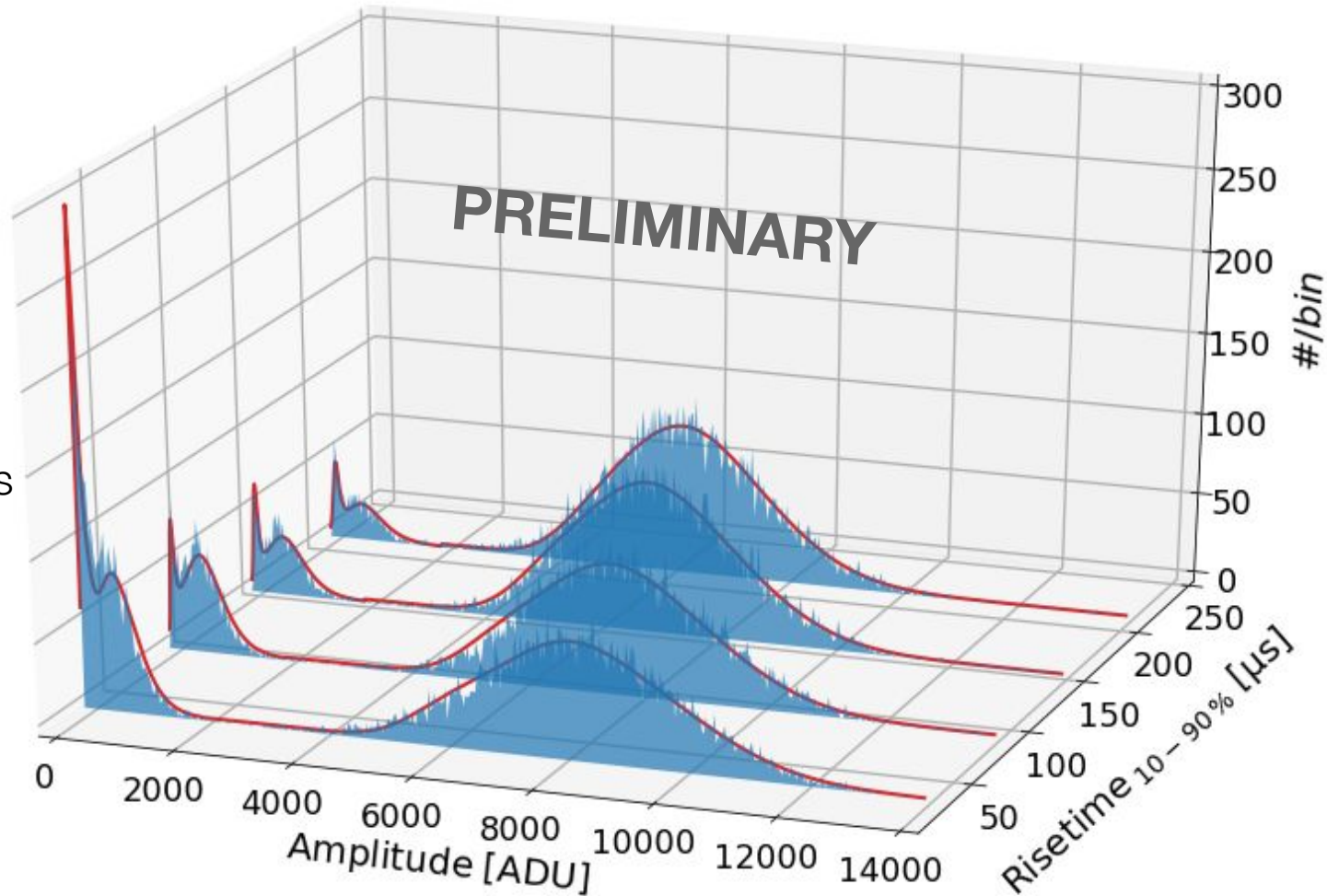
Also used to quantify the performance of the peak-finding algorithm (peak detection threshold and noise trigger probability)

[1] Q. Arnaud et al, Phys. Rev. D 99, 102003 (2019)

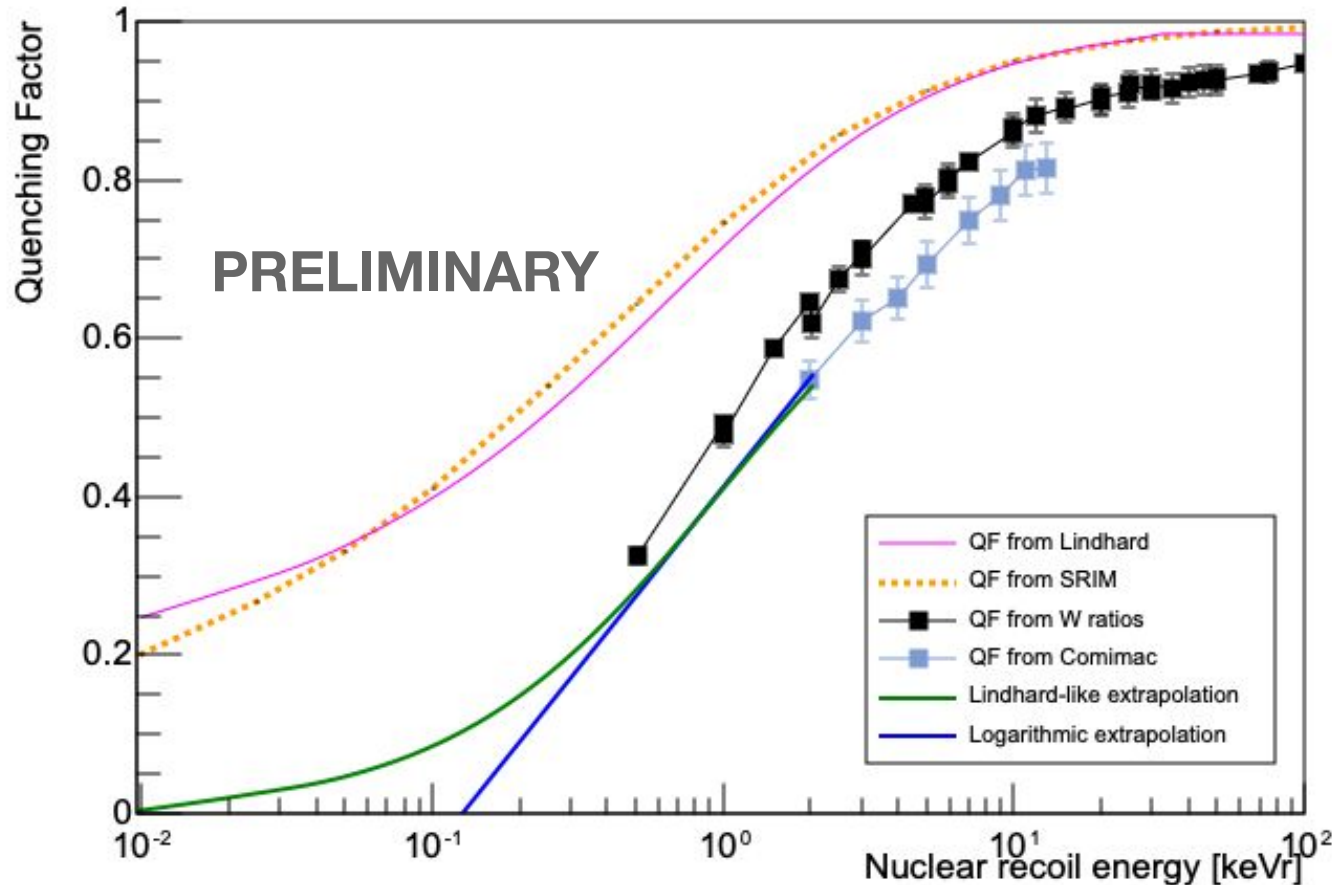
^{37}Ar gas was injected in the SPC after the physics campaign, producing (almost) monoenergetic lines at 200 eV, 270 eV, and 2.8 keV

$$W_0 = 30.0_{-0.15}^{+0.14} \text{ eV}, \quad U = 15.70_{-0.34}^{+0.52} \text{ eV}, \quad F = 0.43 \pm 0.05$$

- Confirmation of energy linearity
- Measurement of the gain of all south-channel anodes
- In situ measurements of the W-value and Fano factor
- Parameterization of electron attachment



Quenching Factor of H in CH4



Quenching factor values from existing W-value measurements for ions [1] and measurements from COMIMAC [2]

The (more conservative) logarithmic extrapolation was used

[1] I. Katsioulas et al, *Astropart. Phys.* 141, 102707 (2022)

[2] L. Balogh et al, *Eur. Phys. J. C* 82, 1114 (2022)

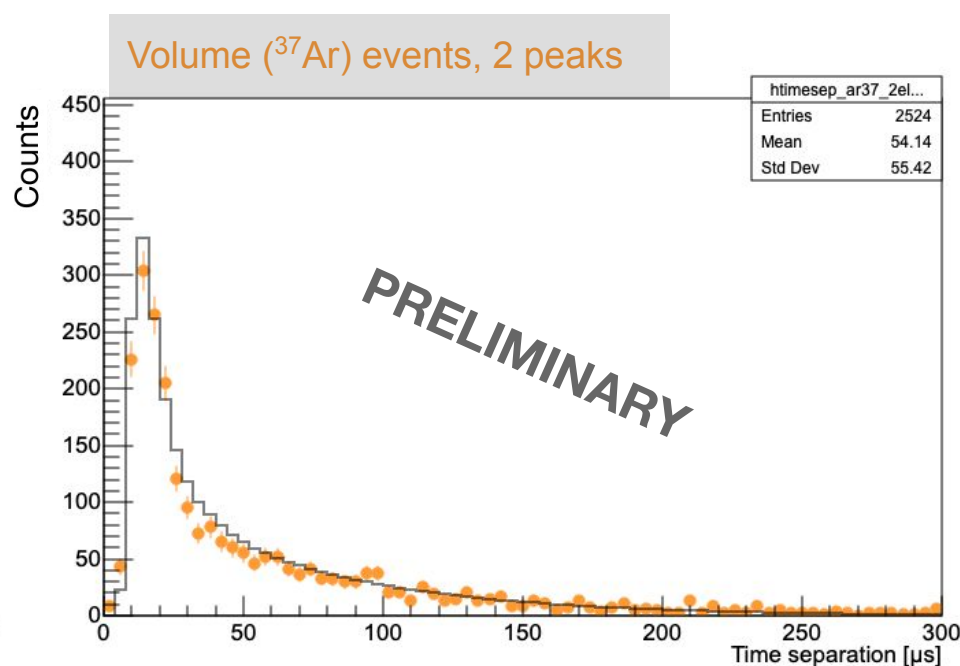
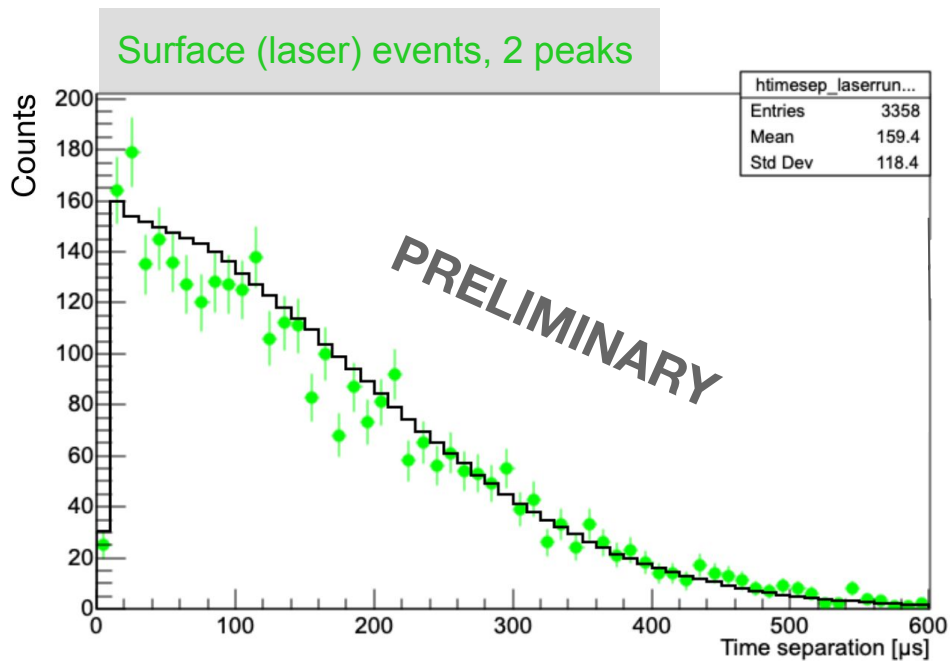
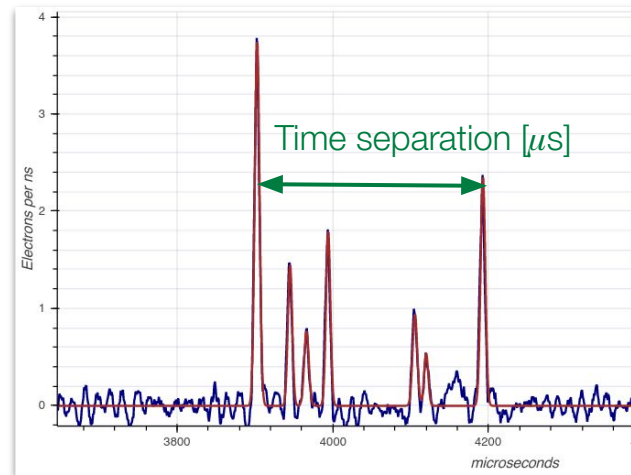
Time separation

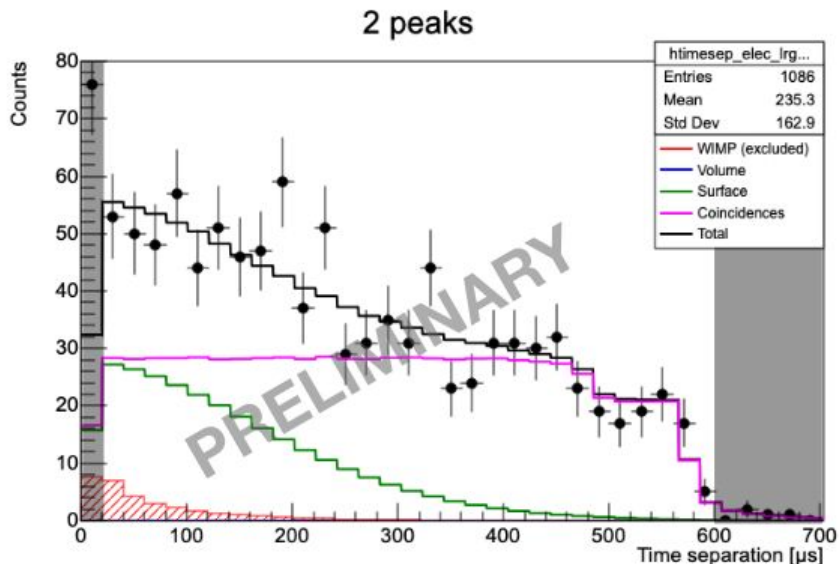


Time separation between the first and last peak is used as the primary analysis variable

Allows for discrimination between surface, volume, and pile-up events

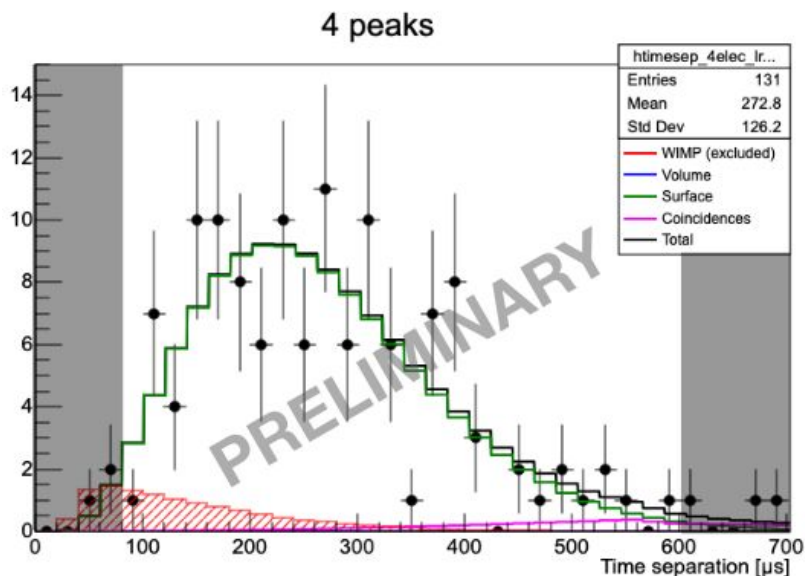
Calibrated with laser (surface) and ^{37}Ar (volume) data





Data divided into subsets with 2/3/4 peaks found (not electrons). The 1 peak signal was overwhelmed by secondary/induced electron events, no fiducialization possible

Time separation (time between first and last peak) is used for surface/volume event discrimination, address coincident event background



The physics data was split into test and blind data (~30/70%); here the fit of the test data is shown, including a WIMP signal component for demonstration (760 MeV/c²)

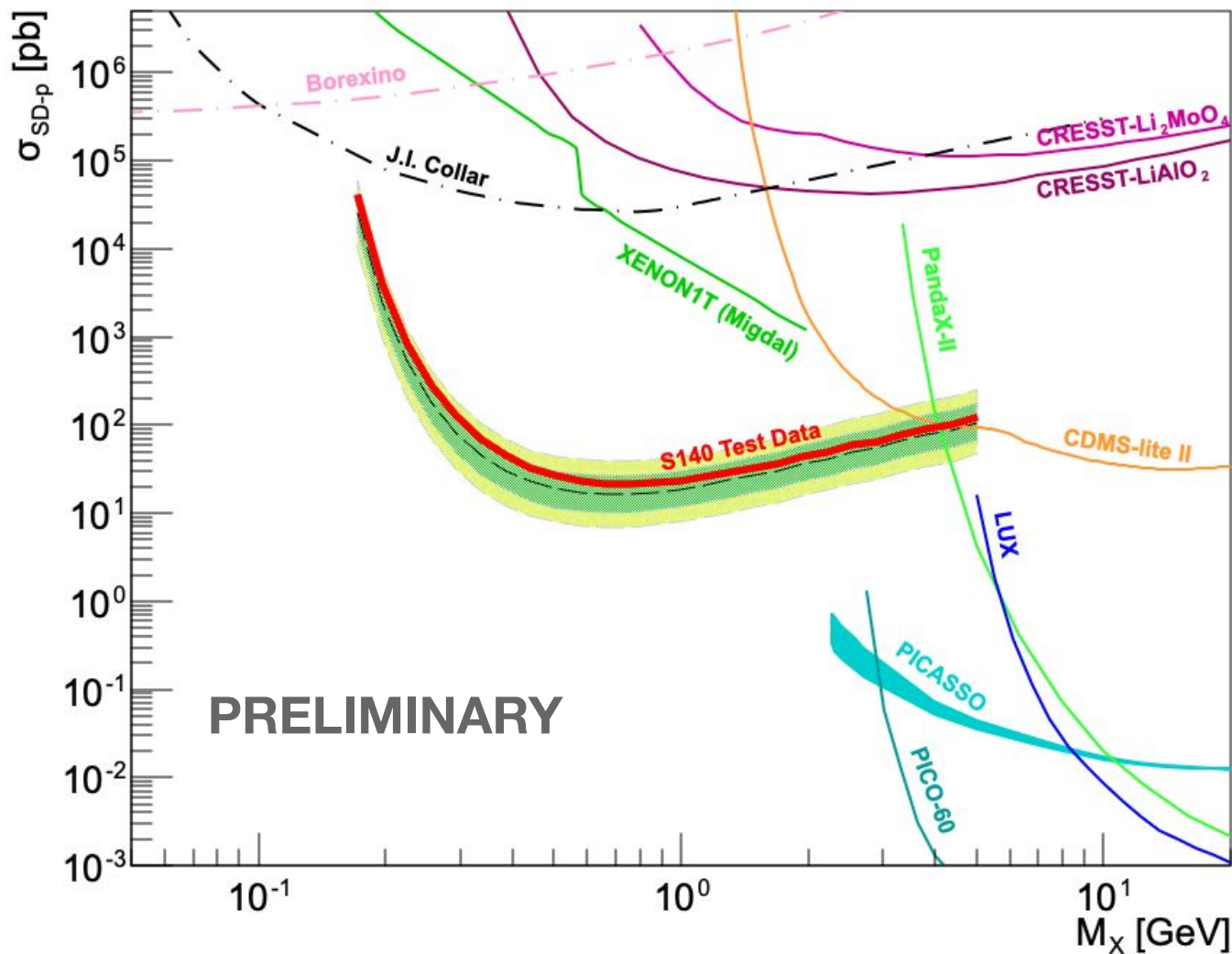
No significant signal observed

WIMP exclusion limit (S140@LSM, 135mbar CH4)

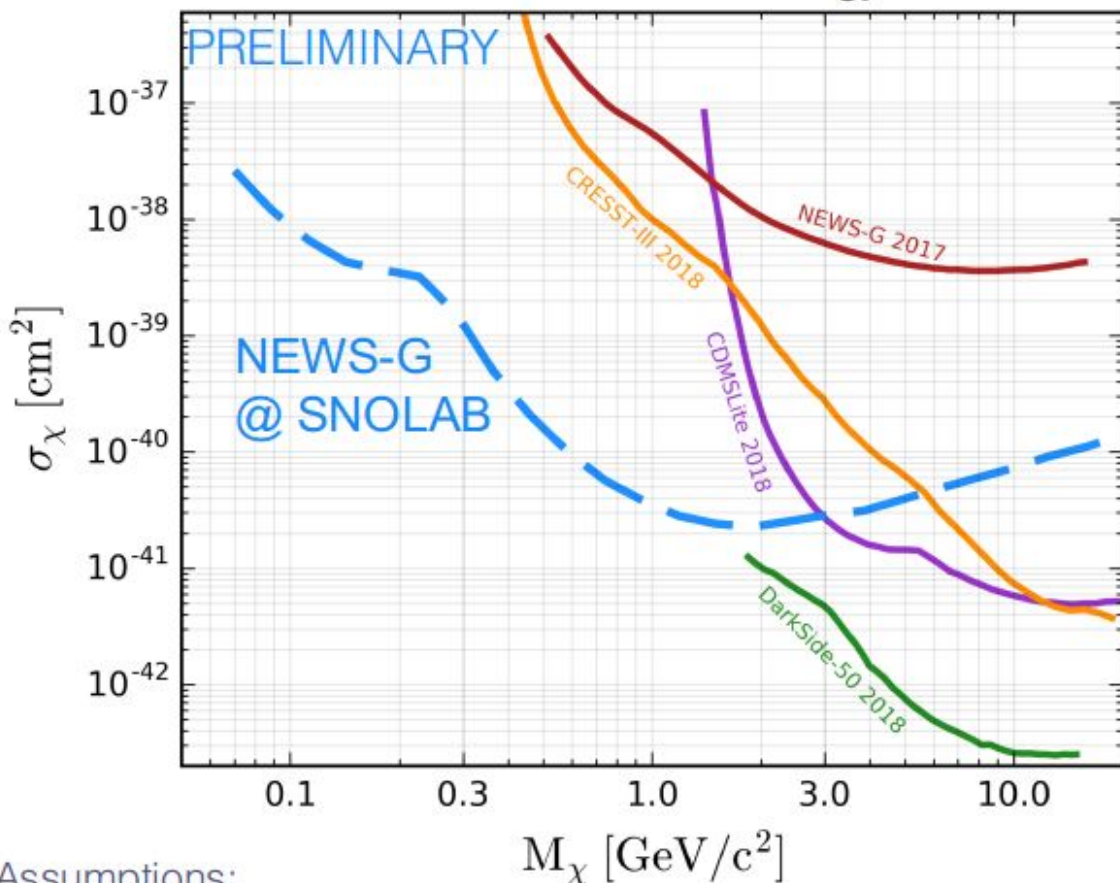
Results with test data
 (~0.12 kg.days)

Profile likelihood ratio method used to calculate 90% exclusion limit on the existence of WIMPs

Full results with blind data expected within weeks - possibly best constraints on SD-p WIMP interactions below 1 GeV!



Expected to be sensitive to WIMP masses ~ 100 MeV using H-rich gas and an energy threshold < 50 eV_{nr}



The new SPC has been installed at SNOLAB, commissioning ongoing!



Assumptions:

Ne + 10% CH₄, Exposure: 20 kg days, $F = 0.2$, $\theta = 0.12$, SRIM quenching factor, Background: 1.78 dru, ROI: 14 eV_{ee} - 1 keV_{ee}, Optimum Interval Method

1) SNOGLOBE

\varnothing 140 cm
 99.99% Cu
 500 μ m EFCu Layer

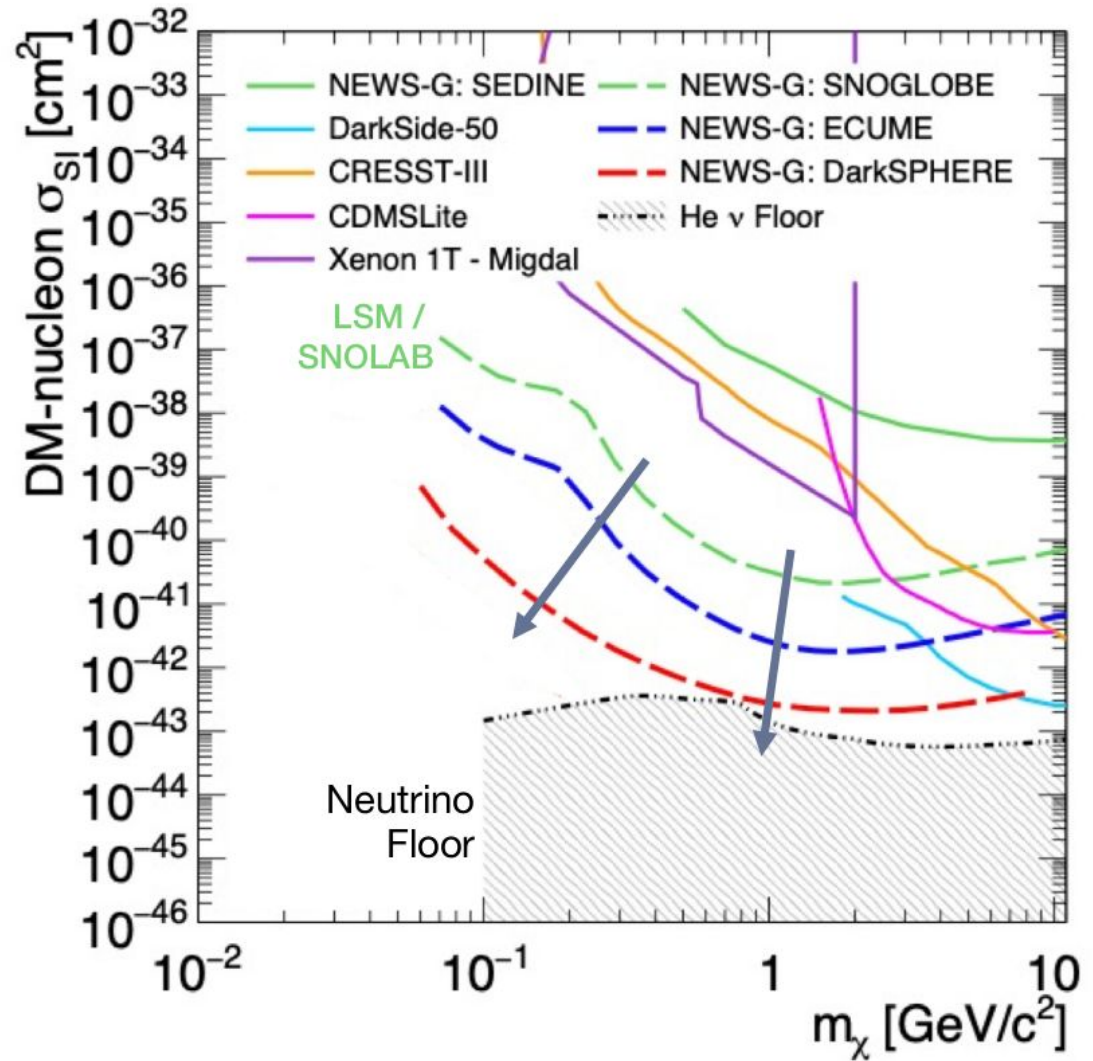
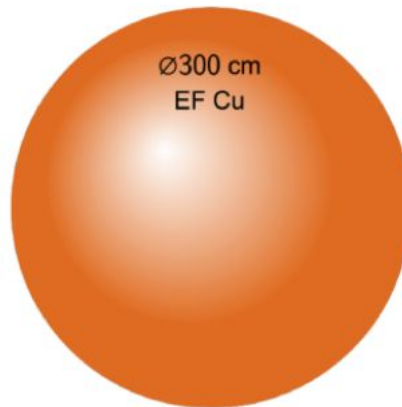


2) ECuME

\varnothing 140 cm
 EF Cu



3) DarkSPHERE



Thank you for your attention!



UNIVERSITY
OF ALBERTA



UNIVERSITY OF
BIRMINGHAM



Queen's
UNIVERSITY

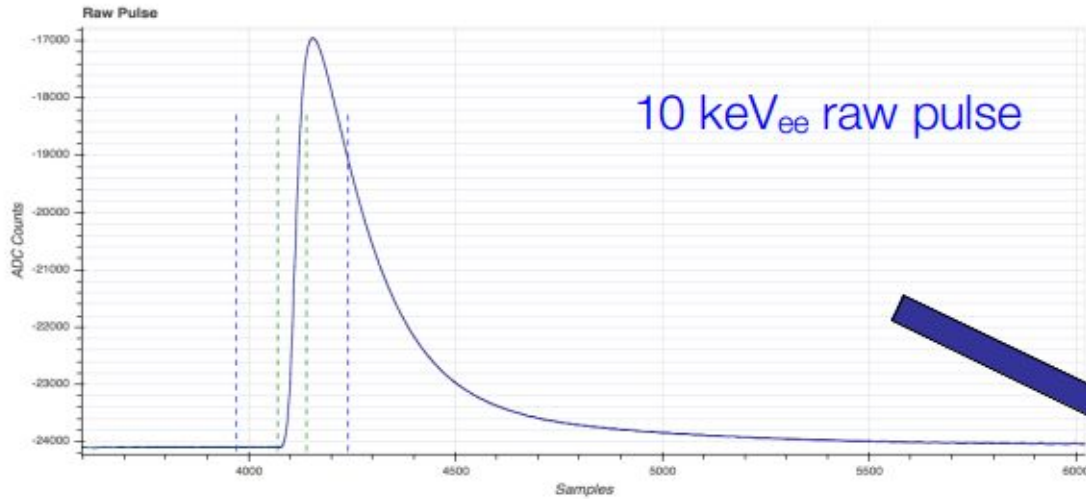


ARISTOTLE
UNIVERSITY OF
THESSALONIKI

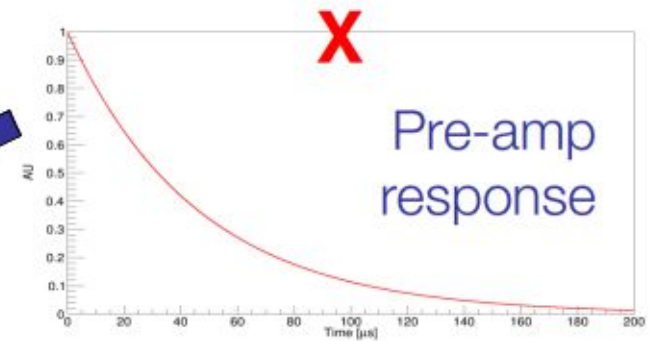
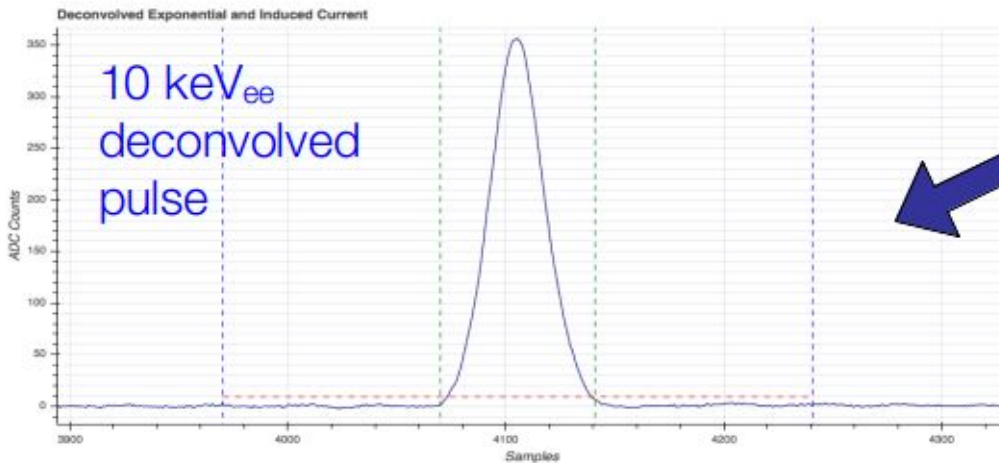
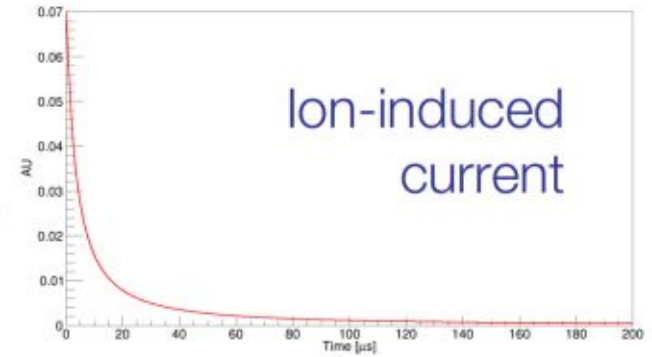


Extra slides

Event reconstruction



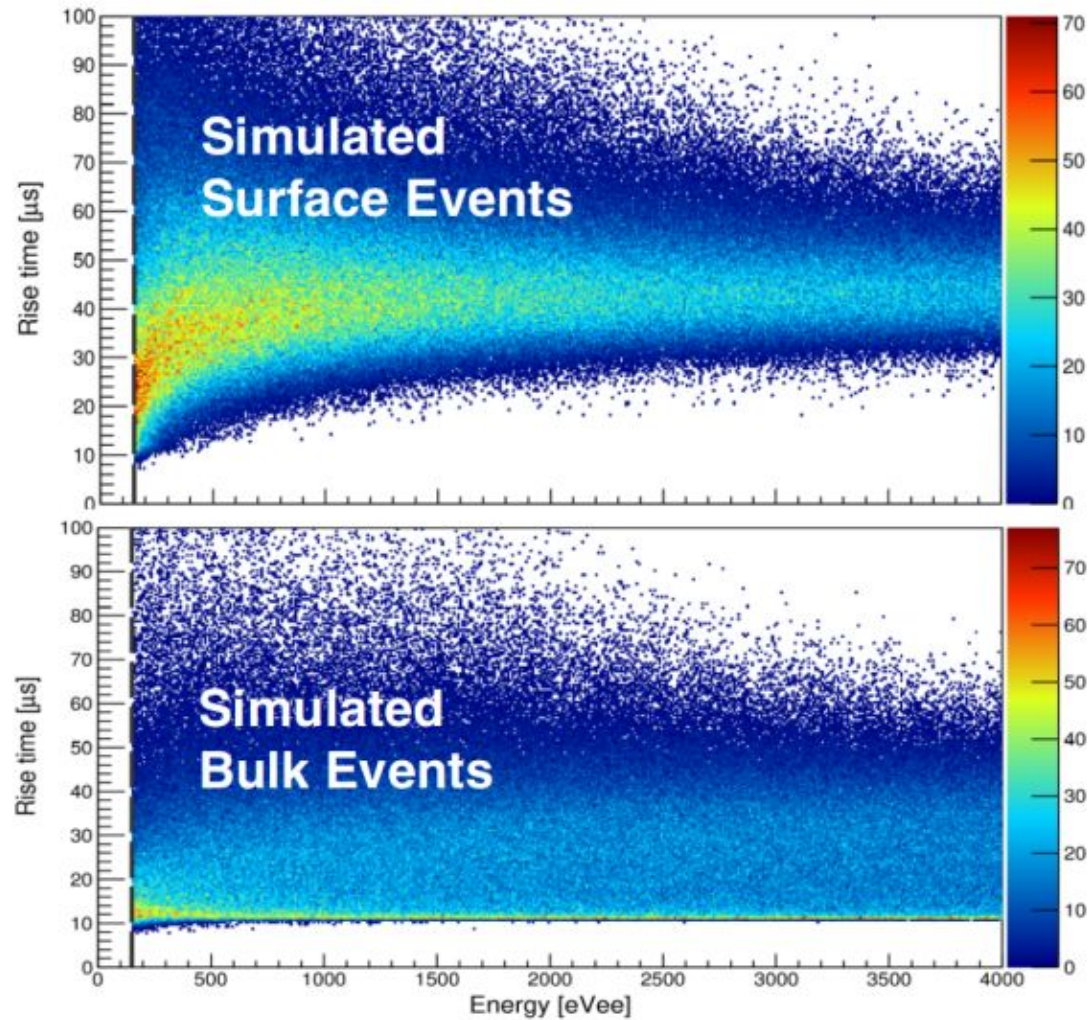
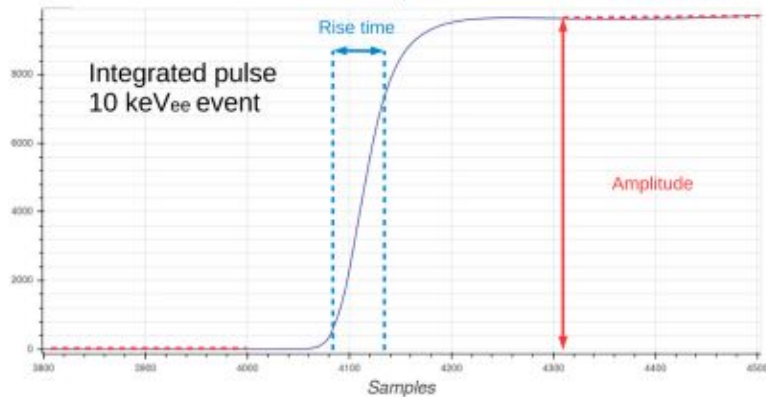
Deconvolve for amplifier response and ion-induced current



Gaussian dispersion in arrival time due to diffusion of charges:

$$\sigma(r) = \left(\frac{r}{r_{sphere}} \right)^3 \times 20\mu s$$

Rise time used for surface event discrimination

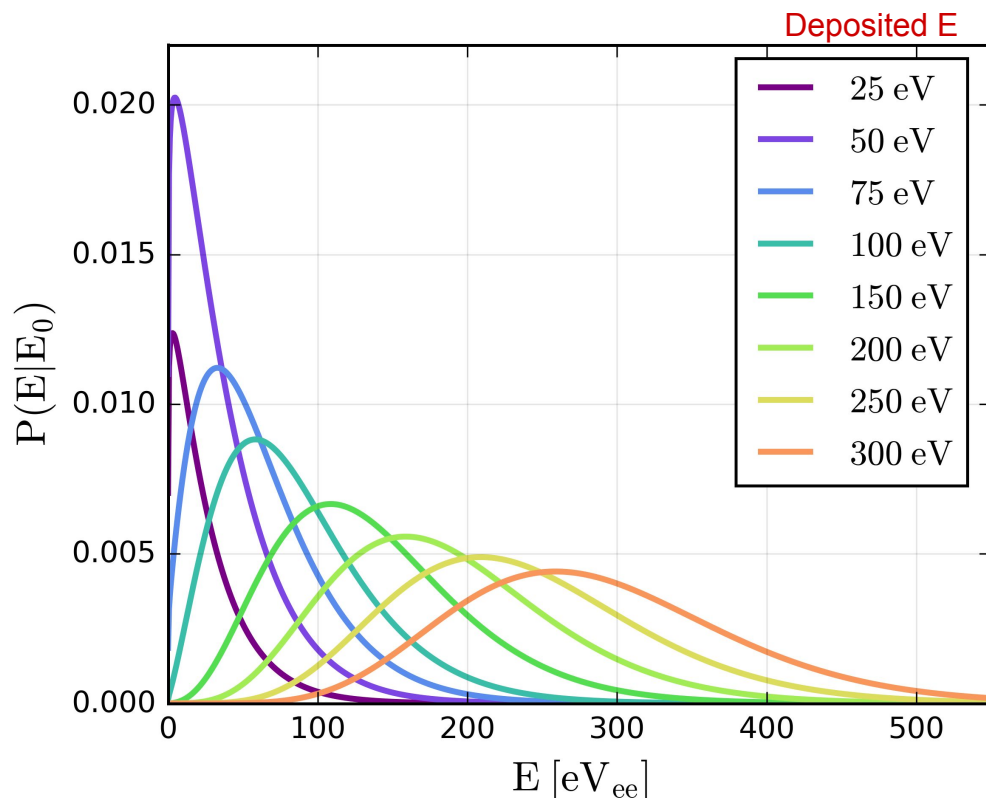


Q. Arnaud et al. (NEWS-G), *Astropart. Phys.* 97, 54 (2018).



Energy response model

The energy response of an SPC can be divided into two main components:



Primary ionization:

- Statistics modelled with COM-Poisson
- Dispersion controlled by Fano factor F

D. Durnford et al, Phys. Rev. D 98, 103013 (2018)

Avalanche (secondary) ionization:

- Statistics modelled with Polya distribution with shape parameter θ
- Mean reconstructed amplitude of 1 primary electron (1000s of avalanche pairs) is $\langle G \rangle$

There's baseline noise on top of the signal, σ_b

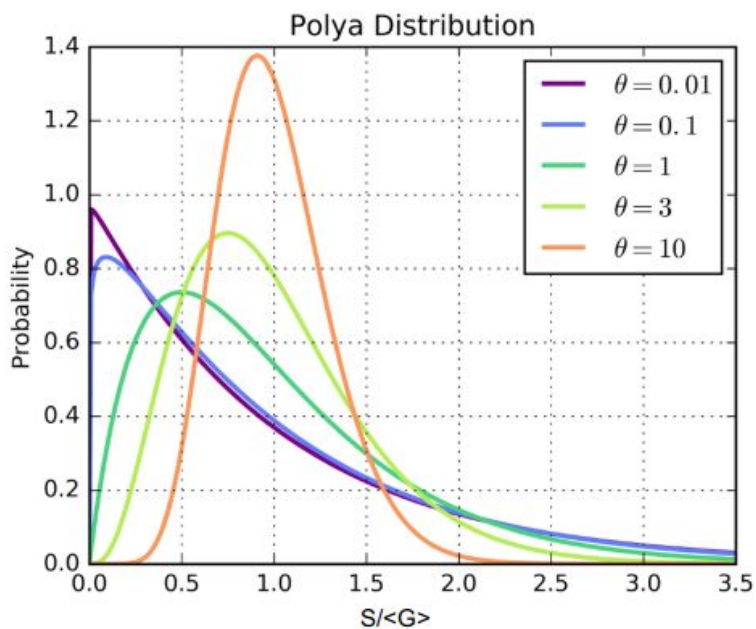
$$\mathcal{F}(E|E_0) = \sum_{n=1}^{n_{\max}} P_{\text{COM}}(n|\lambda(\mu, F), \nu(\mu, F)) \times P_{\text{Polya}}^{(n)}(E|\theta, \langle G \rangle)$$

$$\mu = \frac{E_0 * Q(E_0)}{W(E_0)} \quad n_{\max} = \left\lfloor \frac{E_0}{I} \right\rfloor$$

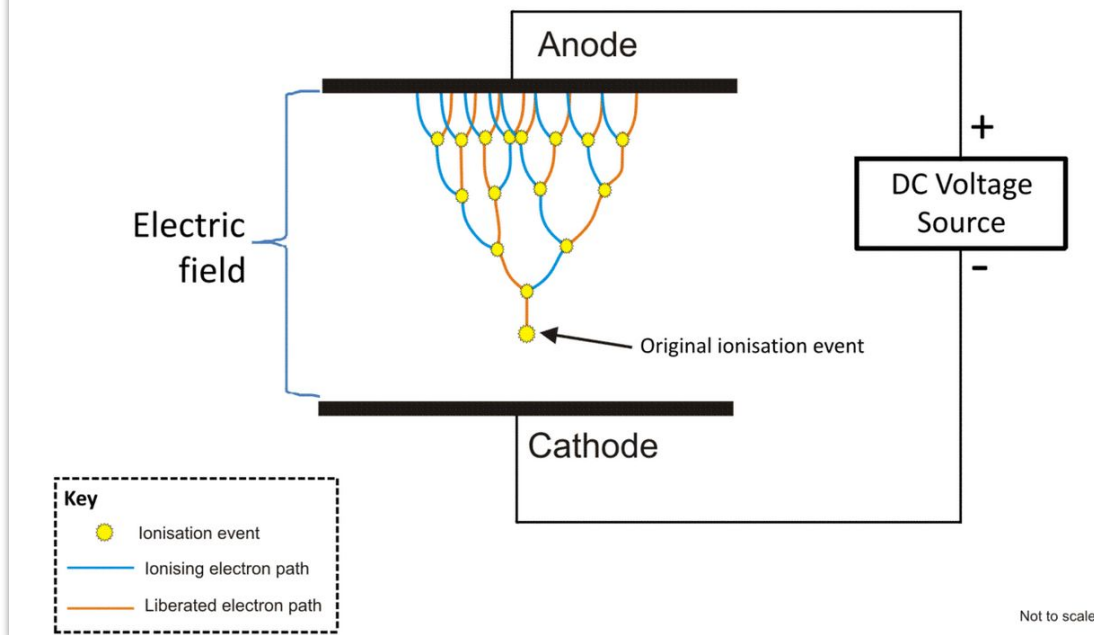
Avalanche response

The distribution of the number of avalanche pairs “S” is approximately exponential

It is known to be well-described by the Polya distribution, with shape parameter θ :



Visualisation of a Townsend Avalanche



$$P_{\text{Polya}}(S | \langle G \rangle, \theta) = \frac{1}{\langle G \rangle} \left(\frac{(1 + \theta)^{1+\theta}}{\Gamma(1 + \theta)} \right) \times \left(\frac{S}{\langle G \rangle} \right)^\theta \exp \left(- (1 + \theta) \frac{S}{\langle G \rangle} \right)$$

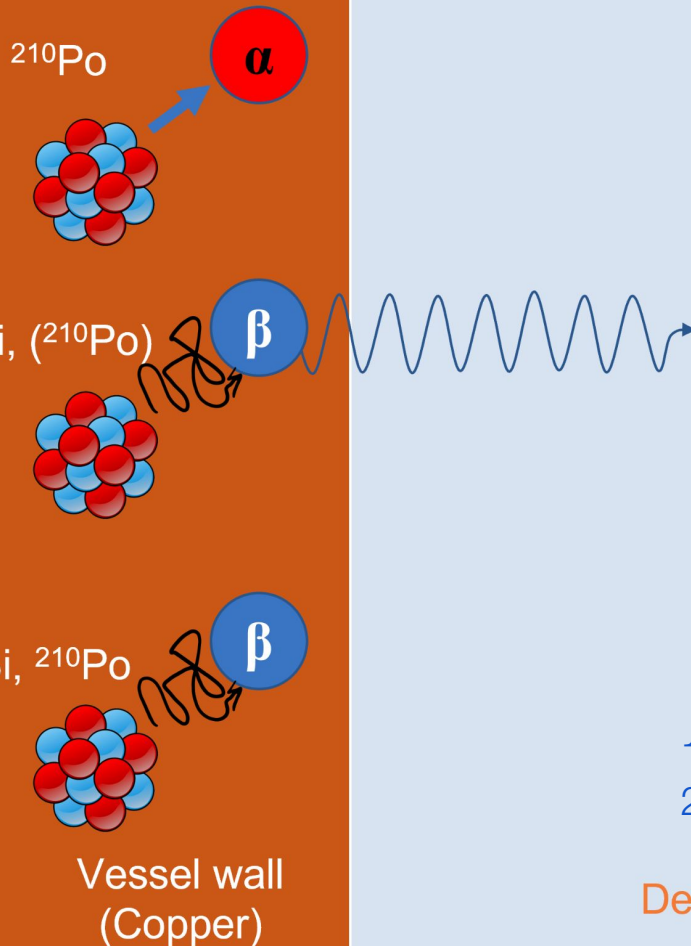
^{210}Pb can be incorporated into copper during the manufacturing process

Bremsstrahlung x-rays ($\sim\text{keV}$) from ^{210}Pb and ^{210}Bi β^- decay in the copper escape, travel through whole gas volume

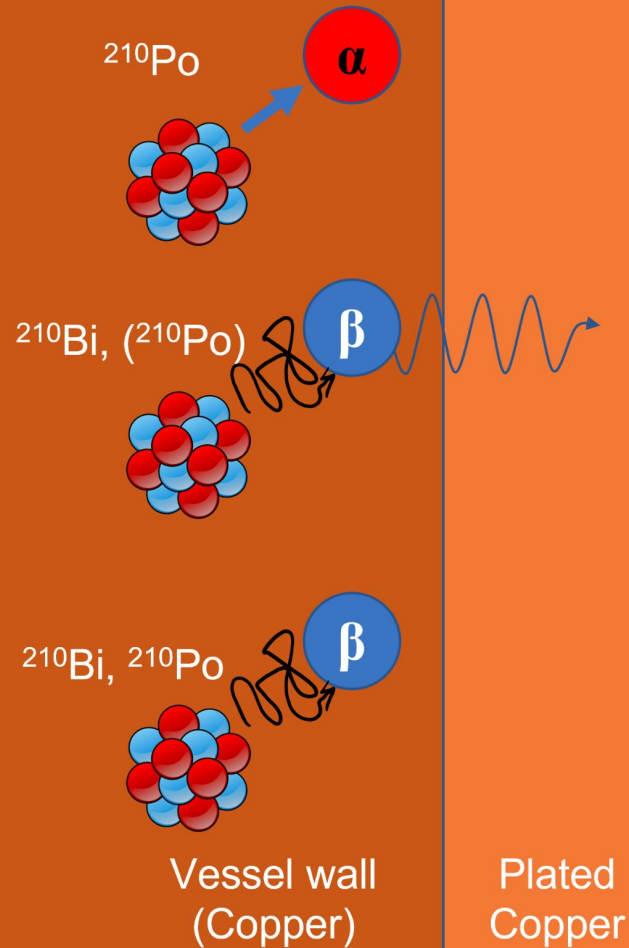
XIA measurements in collaboration with XMASS [1] show 29 ± 8 mBq/kg bulk ^{210}Pb in our copper [2]

1. K. Abe *et al*, Nucl. Instrumen. Methods A, 884 (2018)
2. L. Balogh *et al*, Nucl. Instrumen. Methods A, 988 (2021)

Detector volume



The S140 detector



Plating ~0.5mm of pure copper reduces this background by 70% below 1 keV and 98% overall

Plating successfully carried out at the LSM in collaboration with the Pacific Northwest National Lab



L. Balogh *et al*, Nucl. Instrumen. Methods A, 988 (2021)

Detector volume

Electron peak finding



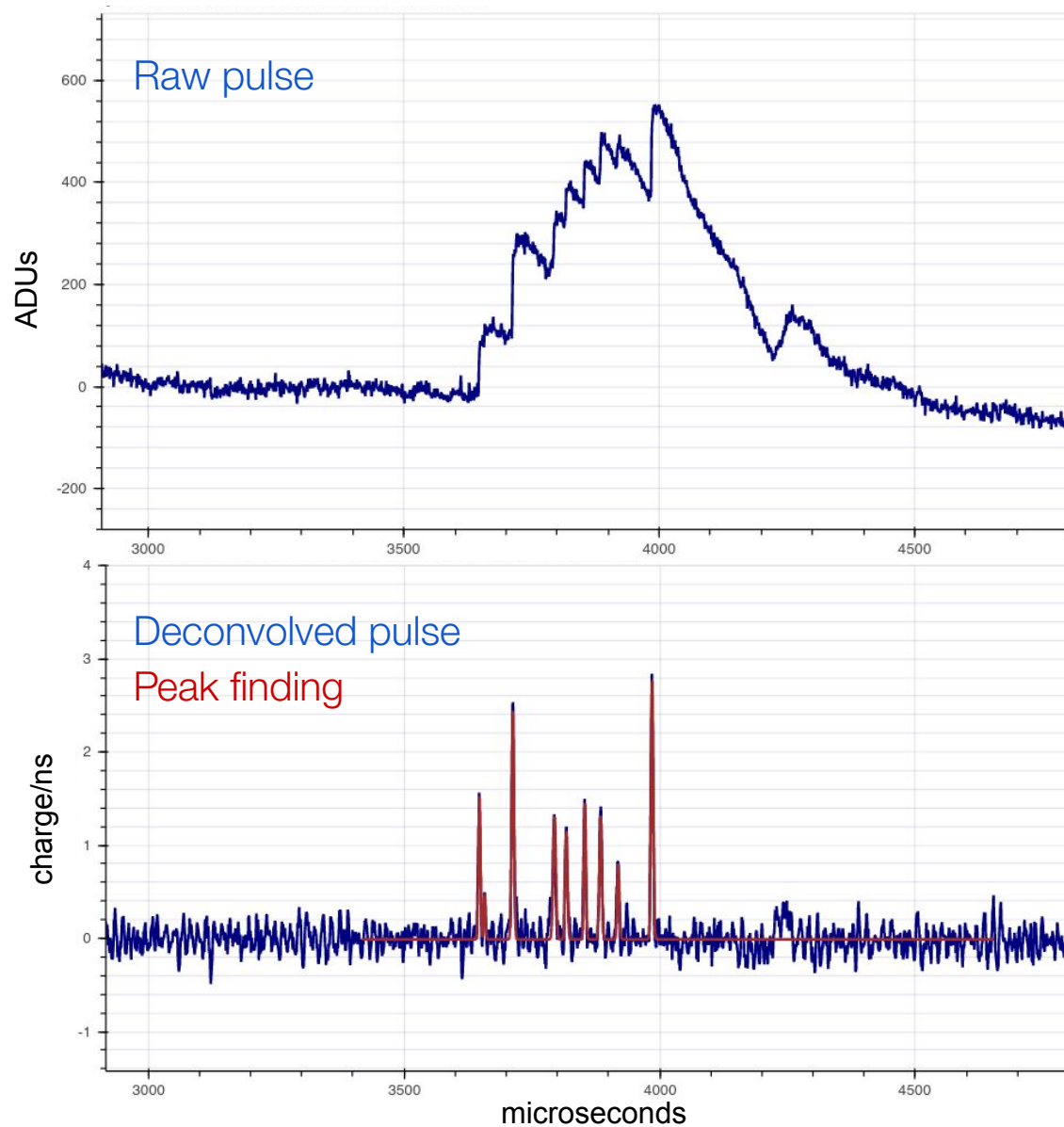
Individual primary electrons are only distinguishable in the deconvolved pulses

Peak finding using ROOT TSpectrum

Single electron efficiency: 60%

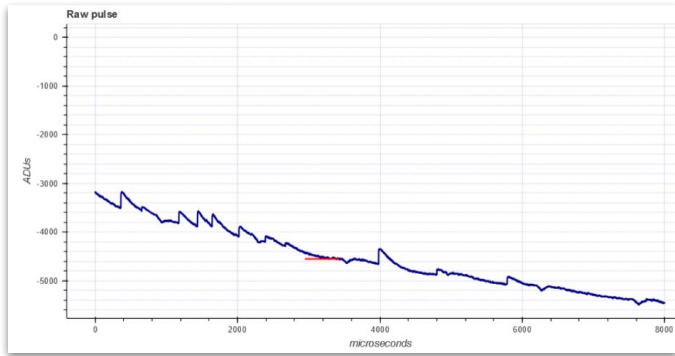
Noise trigger rate: $\sim 10^{-4}$ (in ~ 1.2 ms pulse window)

Ability to separate 100% of peaks greater than $10\mu\text{s}$ apart



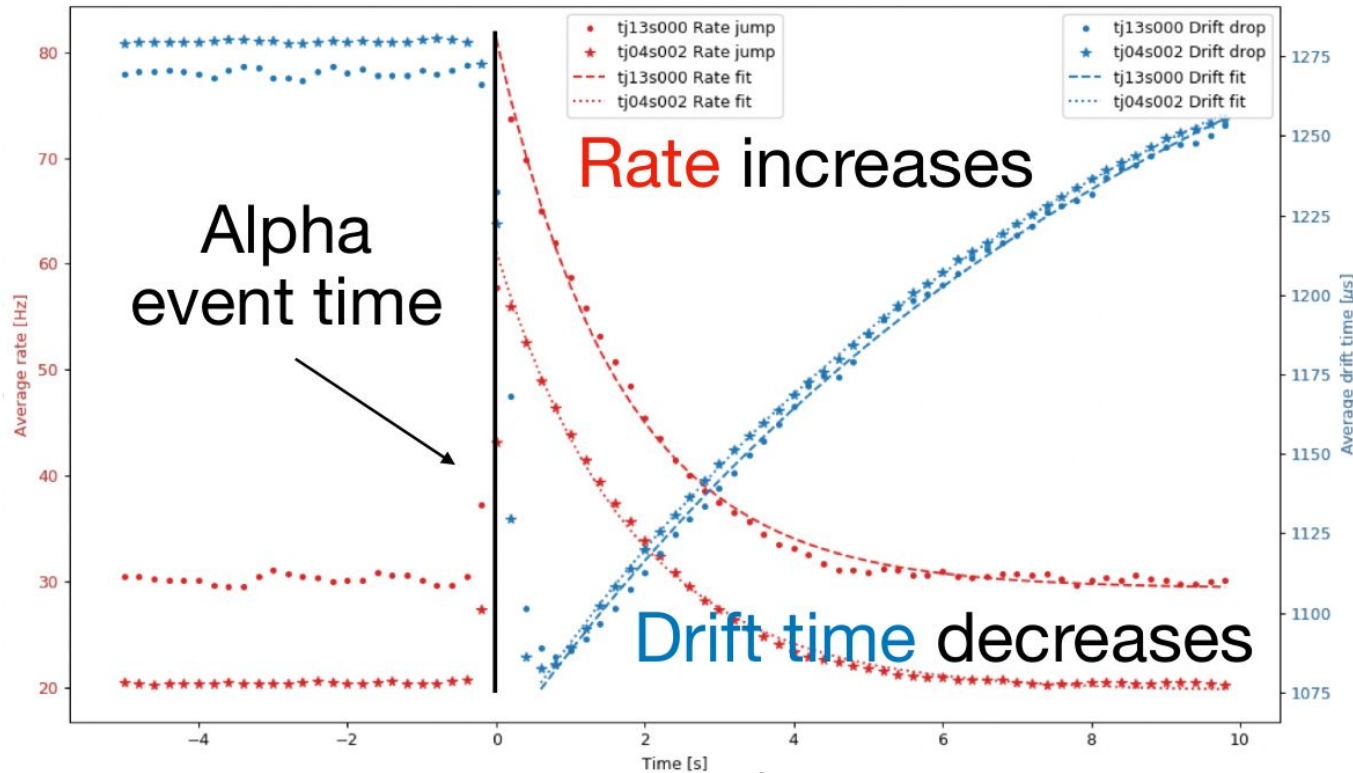


Alpha-induced events



Alpha events (mostly 5.3 MeV Po-210 decays from the surface) produce a large temporary electric field disturbance in the SPC, leading to measurably different electron drift times

They also induce a chain of secondary events for up to 5s afterwards



For the CH_4 analysis, removing 5s after each alpha reduces exposure by 12%, but reduces background rate by ~70%

Pulse shape discrimination

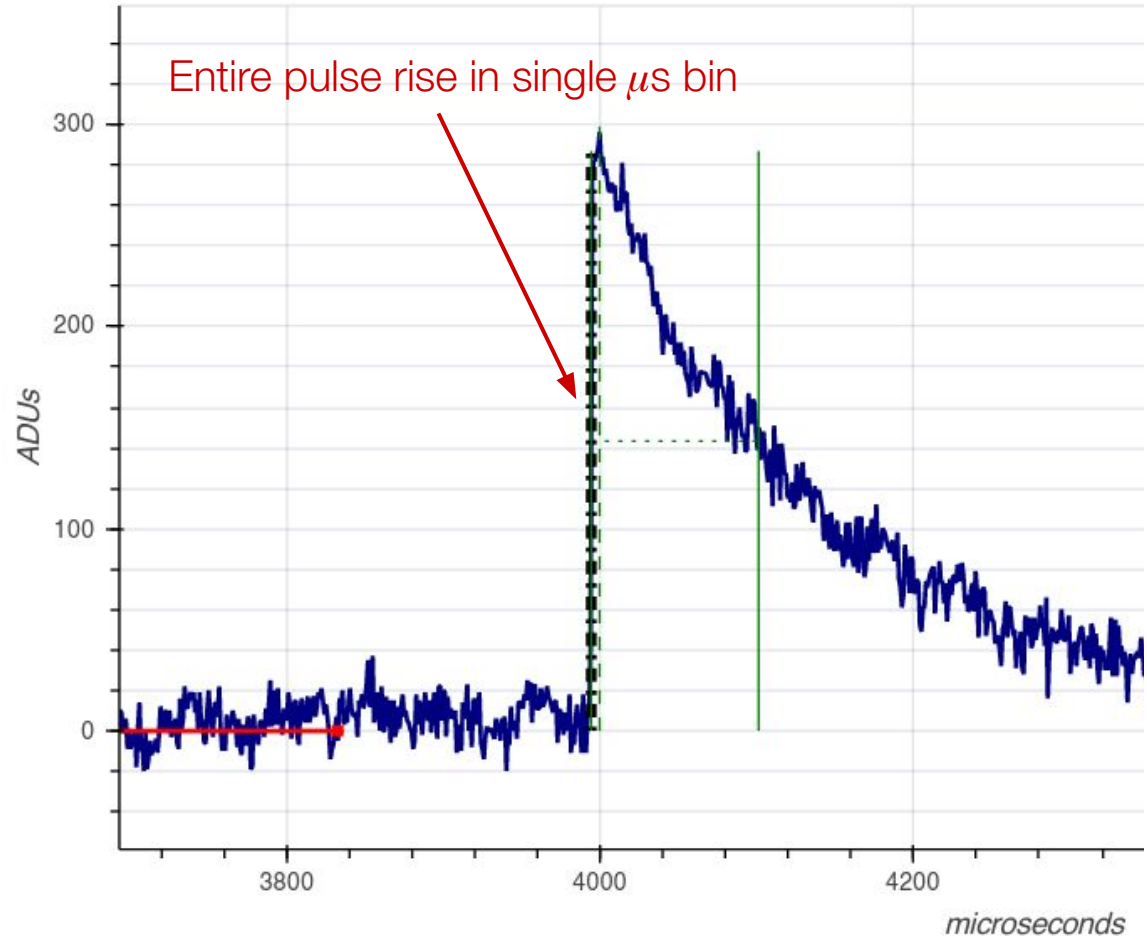


Physical events induce mirror, smaller pulses in the opposite sensor channel with a characteristic scale

Spurious pulses (electronic artifacts) do not exhibit this behaviour, and tend to be sharper

PSD possible using combination of North/South peak amplitudes and pulse derivative (“spikiness”)

Approximately 77% of physical events kept, 95% of spurious pulses rejected



Pulse shape discrimination

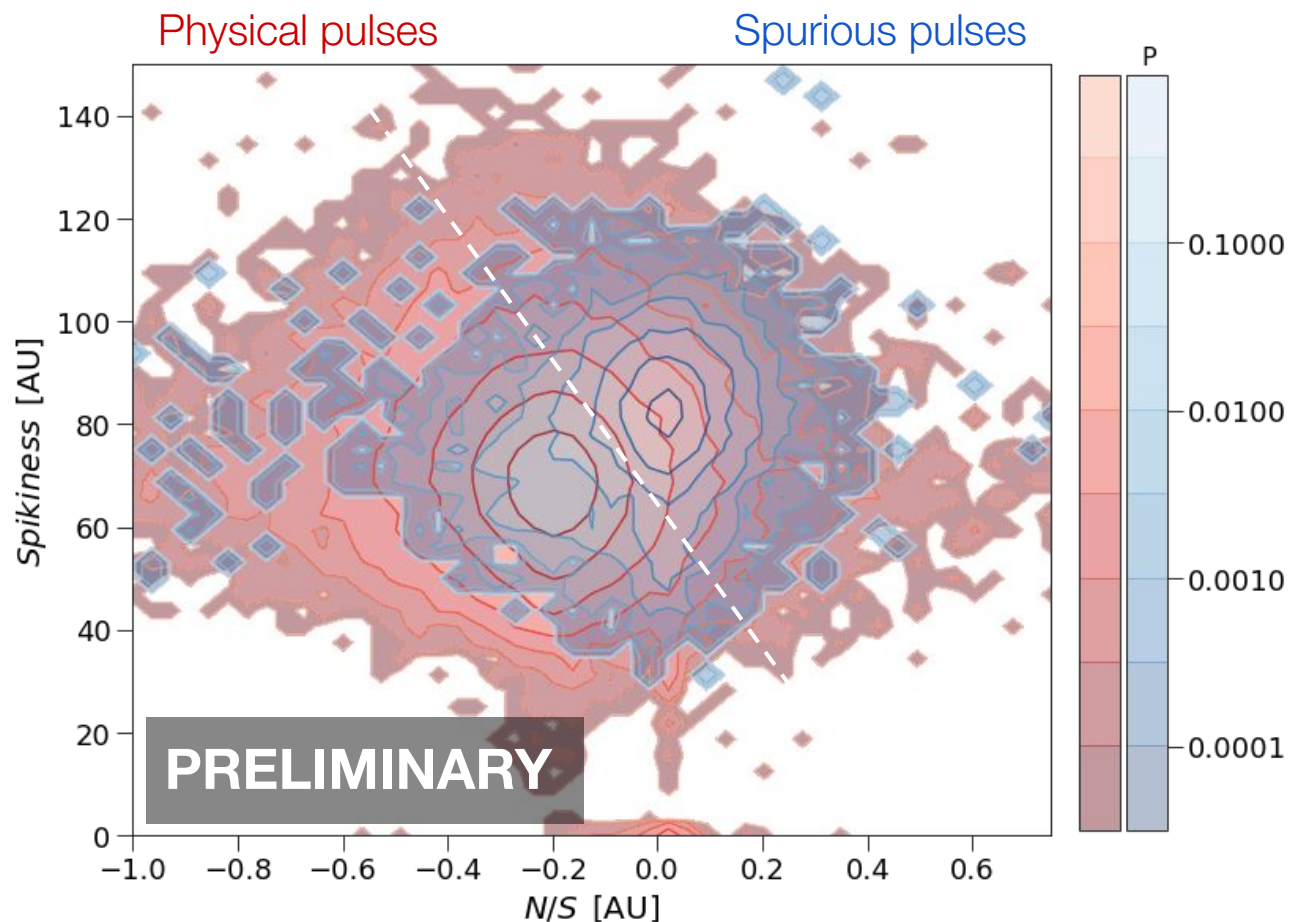


Physical events induce mirror, smaller pulses in the opposite sensor channel with a characteristic scale

Spurious pulses (electronic artifacts) do not exhibit this behaviour, and tend to be sharper

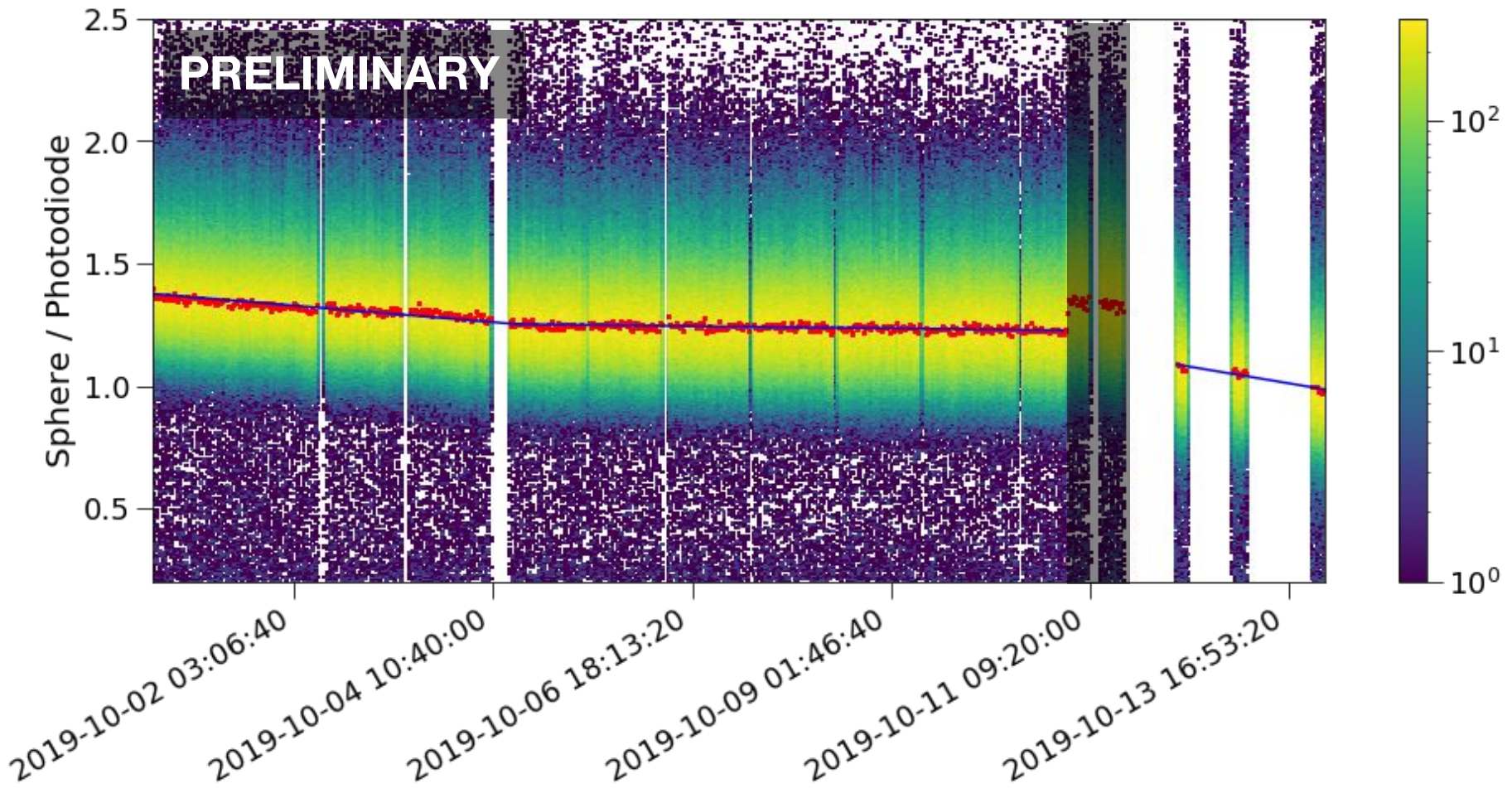
PSD possible using combination of North/South peak amplitudes and pulse derivative (“spikiness”)

Approximately 77% of physical events kept, 95% of spurious pulses rejected



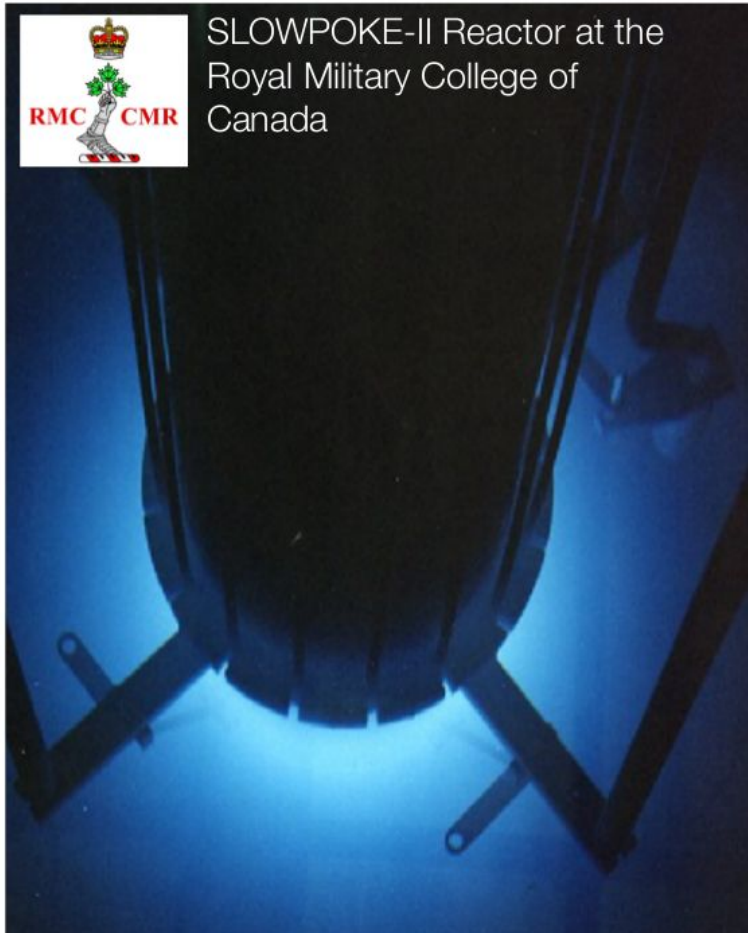
Another purpose is to monitor changes in detector response over time: there is a linear decrease in gain ($\sim 25\%$) due to gas degradation

Drop in gas quality after introduction of ^{37}Ar

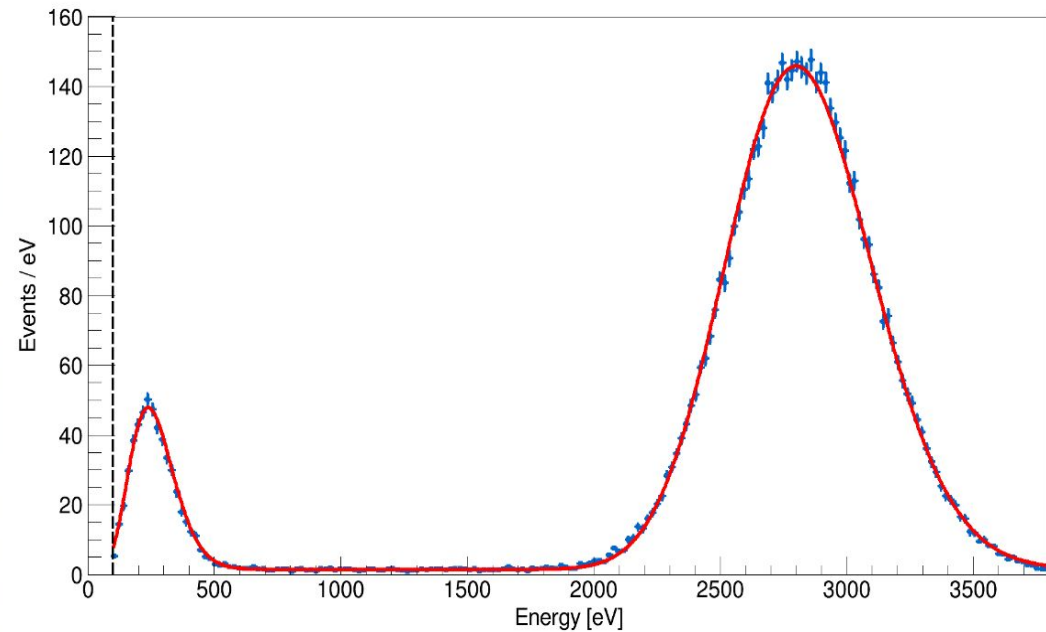


^{37}Ar : radioactive gas that decays via electron capture. But with a 35 day half life, we need a way to produce samples at regularly:

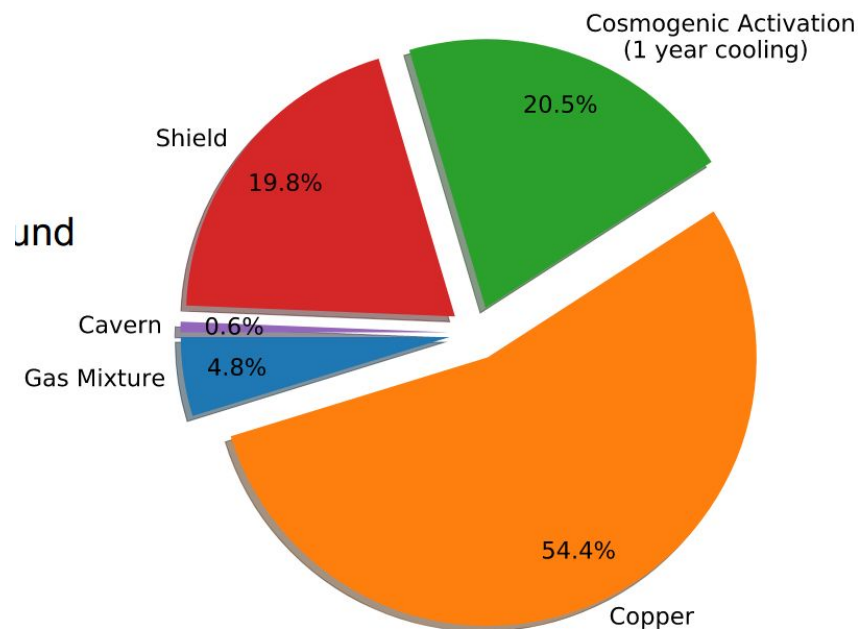
F.G. Kelly et al., *Journal of Radioanalytical and Nuclear Chemistry* 318(1) (2018).



K and L1-shell decays produce low energy x-rays and auger electrons uniformly throughout the detector



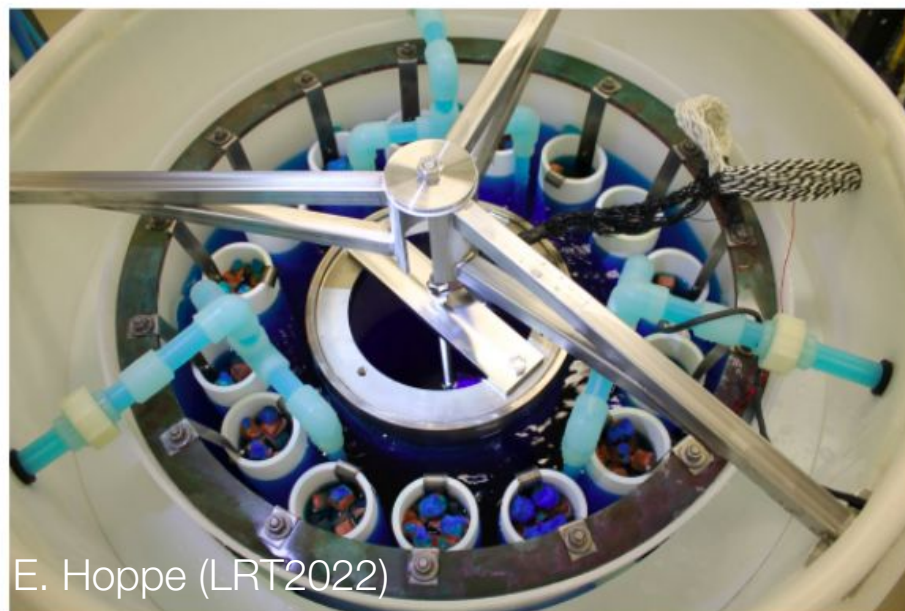
Q. Arnaud et al, *Phys. Rev. D* 99, 102003 (2019)



Despite efforts to self-shield Cu contamination, Pb-210 in the copper remains our largest background

Cosmogenic activation from surface time is also a large component!

The **ECuME** project
(Electroformed Cuprum
Manufacturing Experiment) aims
to develop a copper
electroforming facility in SNOLAB!



E. Hoppe (LRT2022)